ABSTRACT

CHEMICAL REACTIONS AND MASS TRANSPORT IN EMULSION LIQUID MEMBRANE

by
Huifang Fan

Emulsion liquid membrane (ELM) systems are an important technique for wastewater cleanup. For this purpose, emulsion globules are dispersed in wastewater (external phase), each emulsion globule consisting of many tiny aqueous droplets (internal phase) enclosed in oil (membrane phase). Hazardous chemicals in the wastewater are transported into the internal droplets by mass transfer mechanisms.

Since Li first invented an ELM system in the 1960s, much research effort has been devoted to experimentally finding the optimal conditions for ELM recovery of various chemicals. Such studies would have benefited greatly from the guidance of mathematical models, especially those that provide analytical predictions. However, mathematical modeling of ELM systems is highly challenging due to the interplay of transport phenomena and chemical reactions.

In carrier mediated mass transfer in an ELM system, the hazardous chemical in the external phase are extracted by reactions at the external-membrane interface to form a complex with the carrier compound in the membrane phase. The complex then diffuses to the internal-membrane interface, where the hazardous chemical is stripped from the complex and the carrier freed.

This thesis establishes a mathematical model of carrier mediated mass transfer in ELM systems. This model yields analytical solution that accurately predicts experimental results. This solution provides theoretical guidance to optimal recovery conditions and maximum achievable recovery efficiency.

Using metal recovery as an example, this thesis conducts a first-principle study of the extraction chemical reactions at the external-membrane and the stripping chemical reactions at the internal-membrane interfaces and derives the extraction and stripping distribution coefficients. This thesis also finds chemical reactions in the internal phase greatly improve equilibrium recovery efficiency but also greatly lengthen the time to reach equilibrium.

The analytical concentration profiles consist of converging series of infinite terms each involving an eigenvalue of a certain eigenvalue equation. When external resistance exceeds internal resistance, this eigenvalue equation exhibits a remarkable singular behavior with significant impact on the concentration profiles. Also remarkable is the metal accumulation phenomenon at the external-membrane interface when internal resistance is big relative to external resistance.

CHEMICAL REACTIONS AND MASS TRANSPORT IN EMULSION LIQUID MEMBRANE

by
Huifang Fan

A Dissertation
Submitted to the Faculty of
New Jersey Institute of Technology
In Partial fulfillment of the Requirements for the Degree of
Doctor of Philosophy

Department of Chemical Engineering,
Chemistry, and Environmental Science

May 1999

APPROVAL PAGE

CHEMICAL REACTIONS AND MASS TRANSPORT IN EMULSION LIQUID MEMBRANES

Huifang Fan

Dr. Ching-Rong Huang, Dissertation Advisor Date
Professor of Chemical Engineering, Chemistry and Environmental Science, NJIT

Dr. Deran Hanesian, Committee Member Date
Professor of Chemical Engineering, Chemistry and Environmental Science, NJIT

Dr. Dana Knox, Committee Member Date
Professor of Chemical Engineering, Chemistry and Environmental Science, NJIT

Dr. Henry Shaw, Committee Member Date
Professor of Chemical Engineering, Chemistry and Environmental Science, NJIT

Dr. Paul Chan, Committee Member Date
Professor of Civil Engineering, NJIT

BIOGRAPHICAL SKETCH

Author: Huifang Fan

Degree: Doctor of Philosophy

Date: May 1999

Undergraduate and Graduate Education:

- Doctor of Philosophy in Chemical Engineering,
  New Jersey Institute of Technology, Newark, NJ, 1999
- Master of Science in Civil Engineering
  Tianjin University, Tianjin, P. R. China, 1990
- Bachelor of Science in Thermal Engineering,
  Harbin Architectural and Civil Engineering University, Harbin, P. R. China
  1988

Major: Chemical Engineering

Presentations and Publications:

E. H. Wu and H. F. Fan, *"The Study on the Defluoridation of Activated Fluorite,"* Proceedings of the XXth Conference of the International Society for Fluoride Research, (ISFR'94), Beijing, 1994

This Dissertation is dedicated to my parents, my husband and my son

ACKNOWLEDGMENT

I am deeply grateful to my thesis advisor, Professor Ching-Rong Huang, whose profound scientific insights and rigorous research style are the inspiration to this project. Even on sick bed he continued to provide guidance to me on the project. I am extremely fortunate to have such a mentor.

I also wish to express my heartfelt thanks to my committee members, Professor Paul Chan, Professor Deran Hanesian, Professor Dana Knox and Professor Henry Shaw, for their precious time and valuable help. Professor Shaw gave me many excellent suggestions on this project. Professor Knox taught me a lot about thermodynamics. Professor Hanesian took upon himself the onus of correcting the grammar, style and format of the entire thesis. He also gave me many excellent suggestions on the presentation and organization of the thesis. His special kindness is greatly appreciated.

I owe special thanks to Professor Basil Baltzis for his guidance and patience during our collaboration and his advice and help afterwards. I am also indebted to Professor Gordon Lewandowski for his advice, encouragement and help. I thank Professor Norman Loney for his guidance, encouragement and friendship. I also thank Professor Robert Barat for his helpful advice.

I thank Cynthia Wos and Peggy Schel for much kind help. I thank Clint Broadway from whom I learned a lot of experimental techniques.

I thank Annette Damiano for her kind help with my thesis format and help advice.

Graduate study and research are immensely challenging to everyone and especially so to foreign students. I thank Professor Ronald Kane, our Dean of Graduate Studies, for the

countless things he has done to help us overcome difficulties and make our graduate career at NJIT a fulfilling experience.

I thank all my friends for sharing the joys and frustrations of graduate student life and for their encouragement and help.

Finally I thank my loving husband Haiyun for being "the wind beneath my wings". He has a part in almost everything I have accomplished at NJIT. I also thank my little son Frederick whose sweet smile evaporates my weariness from each day's toil and gives new meaning to everything I do. I would like to thank my parents and my sisters who have been the driving force of my striving since I was a little girl.

TABLE OF CONTENTS

Chapter Page

TABLE OF CONTENTS
(Continued)

TABLE OF CONTENTS
(Continued)

Chapter **Page**

LIST OF FIGURES

LIST OF TABLES

NOMENCLATURE

B	Dimensionless emulsion capacity constant, defined as $B=mf'\omega$
b_s	The singular point
b_n	Eigenvalues, n=1,2,3…
C_e	Solute concentration in the external phase (mol/l)
C_e^*	Solute concentration in the external phase on external-membrane interface (mol/l)
C_{e0}	Initial solute concentration in the external phase (mol/l)
$C_{e\infty}$	Solute concentration in the external phase when time goes to infinity(mol/l)
c_i	the concentration of ionic species (mol/l)
C_i	Solute concentration in the internal phase or concentration of metal ion in the internal phase (mol/l)
C_{is}	concentration of metal salt in the internal phase (mol/l)
C_{it}	total concentration of metal in the internal phase, $C_{it} = C_i + C_{is}$ (mol/l)
C_i^*	solute concentration in the internal phase of the membrane-internal interface (mol/l)
C_m	Solute concentration in the membrane phase (mol/l)
C_{me}^*	solute concentration in the membrane phase at the external-membrane interface (or at $r = R$) (mol/l)
C_{mi}^*	solute concentration in the membrane phase of the membrane-internal interface (mol/l)
D_e	Effective diffusivity of solute-carrier complex in the emulsion phase (m^2/sec)
D_i	Diffusivity of solute in the aqueous phase (m^2/sec)
D_m	Diffusivity of solute-carrier complex in the membrane phase (m^2/sec)

NOMENCLATURE
(Continued)

D_s	Static dielectric constant of the solvent
d_I	Diamter of the propeller (m)
d_T	Diameter of the tank (m)
d_{32}	Sauter mean diameter (m)
e	Internal volume fraction of emulsion, defines as $e=V_i/(V_m+V_i)$
f'	Emulsion volume fraction of total volume, defined as $f'=V_m+V_i/(V_e+V_m+V_i)$
$\hat{f}_i$	The fugacity of a component i in a mixture
f_i^0	The fugacity of pure component i at standard state (Henry's law)
G	Ratio of mass transfer resistance of the membrane phase to the external phase, defined as $G=pD_e/Rk$
I	ionic strength of solution, $I = \frac{1}{2}\sum_{i=1}^{n} c_i z_i^2$
k	external mass transfer coefficient (m/sec)
K	Equilibrium constant of chemical reaction
K_γ	Lumped activity coefficient, $K_\gamma = \frac{\gamma_C^c \gamma_D^d}{\gamma_A^a \gamma_B^b}$
K_0	Intermediate variable, defined as $K_0 = \frac{Rkf}{D_e}$
M_B	Molecular weight (g/mol)
N	Total number of emulsion globules during agitating or agitating speed (rps).
p	Extraction distribution coefficient, defined as $C_{me}^* = pC_e^*$

NOMENCLATURE
(Continued)

q	Stripping distribution coefficient, defined as $C_i = qC_m$
r	Radius inside emulsion globule (m)
r_0	ionic radius (m)
R	Sauter mean radius of the emulsion globule (m)
Re	Renold number
T	Absolute temperature
t	Time(sec)
U_e	Dimensionless solute concentration in the external phase, defined as $U_e = \frac{C_e}{C_{e0}}$
U_e^*	Dimensionless solute concentration in the external phase on the external-membrane interface, defined as $U_e^* = \frac{C_e^*}{C_{e0}}$
U_m	Dimensionless solute concentration in the membrane phase, defined as $U_m = \frac{C_m}{pC_{e0}}$
U_m^*	Dimensionless solute concentration in the membrane phase on the membrane-internal interface, defined as $U_m^* = \frac{C_m^*}{C_{e0}}$
V_A	Molar volume of solute A at its normal boiling temperature (cm^3/mol)
V_e	External phase volume (ml)
V_i	Internal phase volume (ml)
V_m	Membrane phase volume (ml)
z_i	Electrical charge or valance

GREEK SYMBOLS

ϕ	Associate factor of solvent (2.6 for water, 1.0 for unassociated solvent)
η_B	Viscosity of solvent phase (cp)
μ	viscosity of the external phase(g/cm/sec)
ρ_s	the density of the solvent (g/cm^3)
ρ	density of the external phase (g/cm^3)
γ	Surfacial tension(dyn/cm)
ν	Dimensionless radius, defined as $= \frac{r}{R}$
τ	Dimensionless time, defined as $\tau = \frac{D_e t}{R^2}$
ω	Intermediate variables, defined as $\omega = 1 - e + eq$ or $\omega = 1 - e + e((1 + K_2[SO_4^{2-}])q)$
γ_i	the activity coefficient of component i

CHAPTER 1

INTRODUCTION

1.1 Emulsion Liquid Membrane (ELM) Systems and Waste Water Treatment

A liquid membrane is an immisible liquid phase separating two mutually miscible liquid phases. In an oil/water/oil (O/W/O) system, an aqueous phase is the liquid membrane separating two oil phases. In a water/oil/water (W/O/W) system, an oil phase is the liquid membrane separating two aqueous phases. This thesis mainly focuses on the W/O/W system.

An emulsion liquid membrane (ELM) system results from mixing two immiscible liquid phases to form an emulsion, and then, by mechanical agitation, dispersing the emulsion in a third liquid phase (external phase). The agitation generates emulsion globules consisting of myriad of internal droplets (internal phase) encapsulated by a membrane phase immiscible to both the internal and external phases. The membrane phase contains an organic compound to stabilize the configuration. This compound is called a surfactant.

This system can separate a variety of chemical compounds by transferring the compound from the external phase through the membrane phase into the internal phase. In the W/O/W system, the external phase is the wastewater to be treated. The hazardous compounds in the wastewater can be transferred into the internal phase. After that the external phase can be separated from the membrane and internal phase. The treated wastewater can be discharged.

Figure 1.1 is an illustration of a process of wastewater treatment using ELM systems.

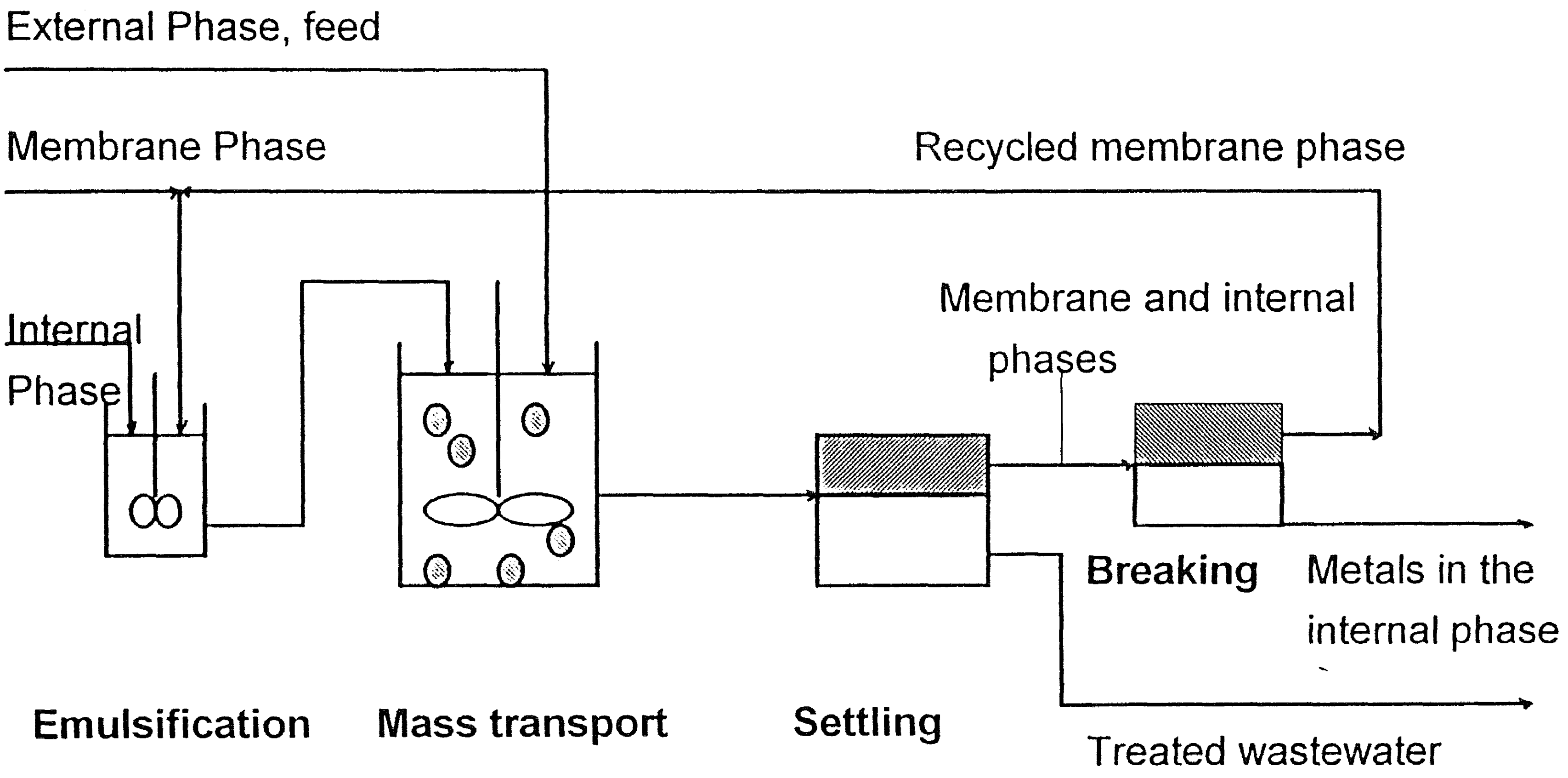

Figure 1.1 Configuration of Process of Emulsion Liquid Membrane Systems

There are four unit operations of this wastewater treatment procedure. The first unit operation is mixing which mixes the internal phase and the membrane phase to form an emulsion. The second unit is emulsification, which mixes the emulsion with the wastewater with an agitator. The emulsion is then present as thousands of globules in the water containing numerous droplets of internal phase. The surfactant in the membrane phase maintains the stability of the globules and droplets and mass transport occurs. The hazardous compound in the wastewater can be transferred into the internal phase. The third unit operation is settling. In this operation the membrane and internal phase are separated from the treated wastewater which has a much lower level of metal concentration than before. The globules regain their form of a continuous phase on the top of the external phase. The last unit is breaking. The membrane phase and the internal phase can be separated with high electric forces. The emulsion, which is rich in hazardous compounds inside the internal phase, is demulsificated and separated by application of high-voltage electric fields (1-2). The membrane phase will be recycled and used again in the emulsification operation. Usually it can only be recycled once (3). This part of the study was not made because of the lack of the equipment.

ELM separation of different compounds has been studied by many investigators in the 1970's and 1980's. Metallic salts which can be treated by ELM have been previously studied. Draxler, Furst and Marr (1988), Draxler and Marr (1986) and Lorbach and Marr (1987) studied zinc (2, 4, 5). Draxler and Marr (1986) studied nickel (4). Marr, Bart and Draxler (1990) studied cadmium, copper, mercury, and lead (6). Fuller and Li (1984) studied chromium (7). Marr and Kopp (1982), Frankenfeld and Li (1977,1979) studied cobalt (8, 9, 10). Reusch and Cussler (1973) (11) , Schiffer et al. (1974) , Culler and Evans (1980) and Bartsch et al. (1987) studied sodium, potassium, lithium, cesium and etc (11, 12, 13, 14). ELM can also treat many organic compounds. Halwachs, Flaschel, and Schugerl (1980); Terry, Li, and Ho (1982), Yan, Huang, and Shi (1987) and Qian, Ma, and Shi (1989) studied organic and inorganic acids (15, 16, 17, 18). Thien, Hatton, and Wang (1986), Ho and Cowan (1987), thien and Hatton (1988) studied acetic and propionic acid, cresol, hydrocyanic acid, etc (19, 20, 21). Thien, Hatton, and Wang (1986), Ho and Cowan (1987) and Thien and Hatton (1988) studied bimolecular (19, 20, 21). Li and Asher (1973) and Asher et al. (1975, 1976, 1979 and 1980) studied amino acid, antibiotics, phospholipids, biomedical reagents, artificial blood cells, cholesterol, toxins and etc (22-26). Among the above applications, removal of zinc from wastewater in the viscose fiber industry and removal of phenol from wastewater have been commercialized in Austria and China respectively (27, 28, 29).

Recently, more work has been done with the ELM system. El-Reefy, Selium, and Aly (1998) studied recovery of uranium (30). Lee, S.S.Wang, and S.D.Wang (1994) studied europium (31). Goto, Kakoi, Yoshii, Kondo and Nakashio (1993) studied rare earth metals (32). Vasconcelos and Carvalho (1993) studied zinc (33). M.S. Uddin and K. Hidajat (1993) studied gold (34). Juang and Lo (1993) studied cobalt (35). Huang and Tsai (1991) studied cobalt and nickel (36). Pickering and Chaudhuri (1997) studied phenylalanine enantiomers (37). Miesiac, Schugerl, Hasler, and Szymanowski (1996) studied penicillin G (38). Juang and Huang (1994) studied Citric Acid, etc (39).

1.2 Mass Tranport Operation in ELM Systems

ELMs were first invented by Norman Li (1970)(40). Figure 1.2 is an illustration of the mass transport operation in ELM. The external phase is the wastewater to be treated. An emulsion globule consists of the membrane phase surrounding many tiny droplets of the internal phase. Mass Transport happens when we mix the external phase with the emulsion phase. The size of the globules depends on the characteristics and concentration of the surfactant in the emulsion, the viscosity of the emulsion, and the intensity and the mode of mixing (41-43). The globule size is controlled in the range of 100 to 200 micrometers in diameter. A large number of the emulsion globules can be formed easily to produce a very large mass transfer area adjacent to the external phase. Each emulsion globule contains many 1 to 3 micrometer internal droplets. Thus, the internal mass transfer area, typically $10^6 m^2/m^3$, is even much larger than the external mass transfer surface area. Therefore, a rapid rate of mass transfer in the ELM process can occur from the external phase to the internal phase. It only takes a few minutes of mixing time to achieve the desired amount of mass transport.

The components of emulsion liquid membrane are:

1. internal phase (receiving phase): an aqueous phase, actually made up of encapsulated droplets, which will receive the solute.
2. external phase (source phase or feed phase): a continuous aqueous phase of wastewater which is the source of the metal ions.
3. membrane phase: an organic phase that separates the internal droplets in the emulsion from the external phase. It usually consists of two components:

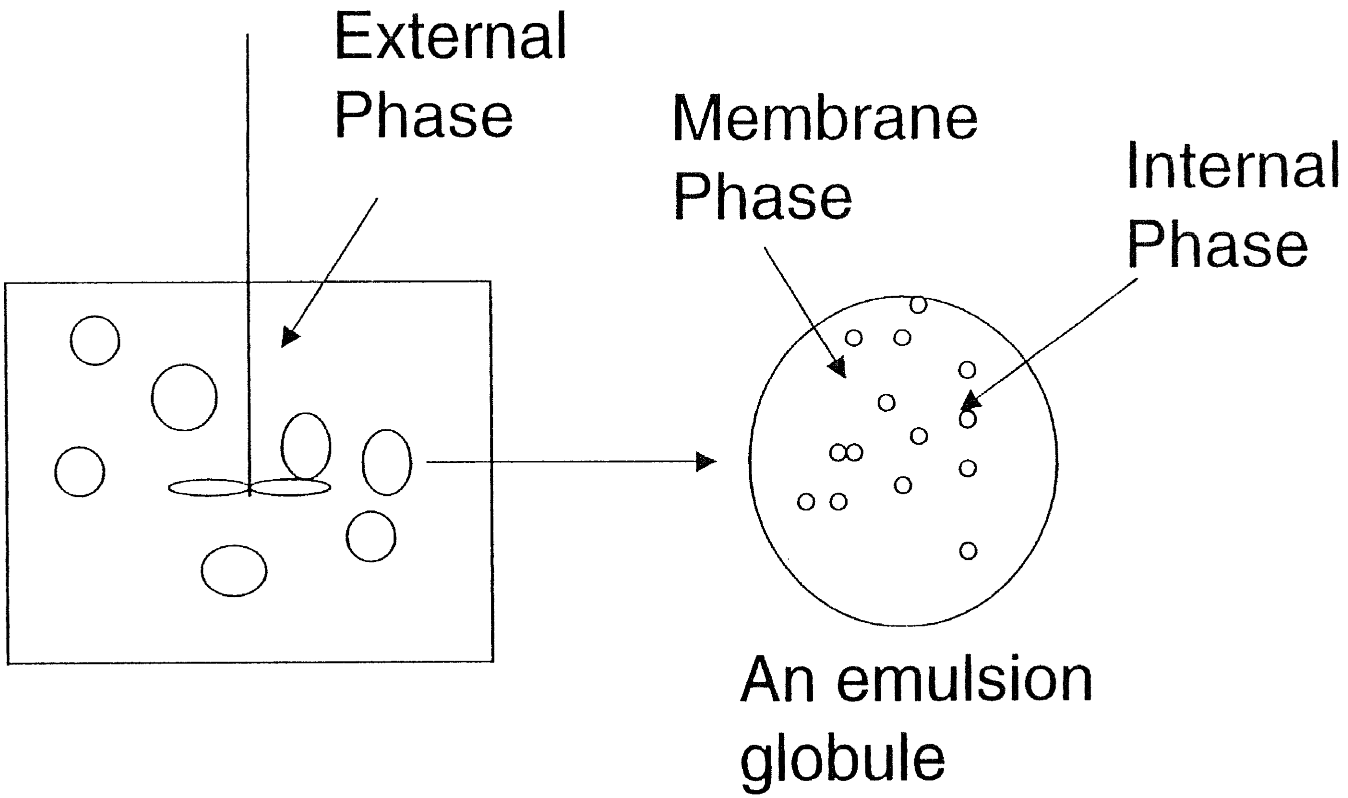

Figure 1.2 Mass Transport Operation of ELM System

a. diluent: organic solvent

b. surfactant: stabilizer of the system

For carrier-facilitated transport which will be discussed later, another compound, an extractant, is added into the membrane phase. The extractant transfers the metal ion from the external phase to internal phase.

There are two types of mechanisms of mass transport: type 1 and type 2 facilitation (44,45,46). In type 1 facilitation, the reaction in the internal phase of the ELM maintains a solute concentration of effectively zero. This is the minimization of the diffusing solute species in the internal phase. The reaction of the diffusing species with a chemical reagent in the internal phase forms a product incapable of diffusing back through the membrane. The driving force of the diffusion of the desired compound from external phase to internal phase is the concentration difference. Extraction of phenol is a good example.

In type 2 facilitation, also called carrier-facilitated transport, the diffusing species are “carried” across the membrane phase by a “carrier” compound, extractant. Reaction of the diffusing species and the carrier compound takes place both at the external interface, between external and membrane phases, and the internal interface, between the membrane and internal phases. In this thesis, all the systems belong to type 2 facilitation. Metal recovery usually uses this type of facilitation. This study focuses on metal recovery with type 2 facilitation.

Figure 1.3 gives the mechanism of mass transport of type 2 facilitation using copper as an example.

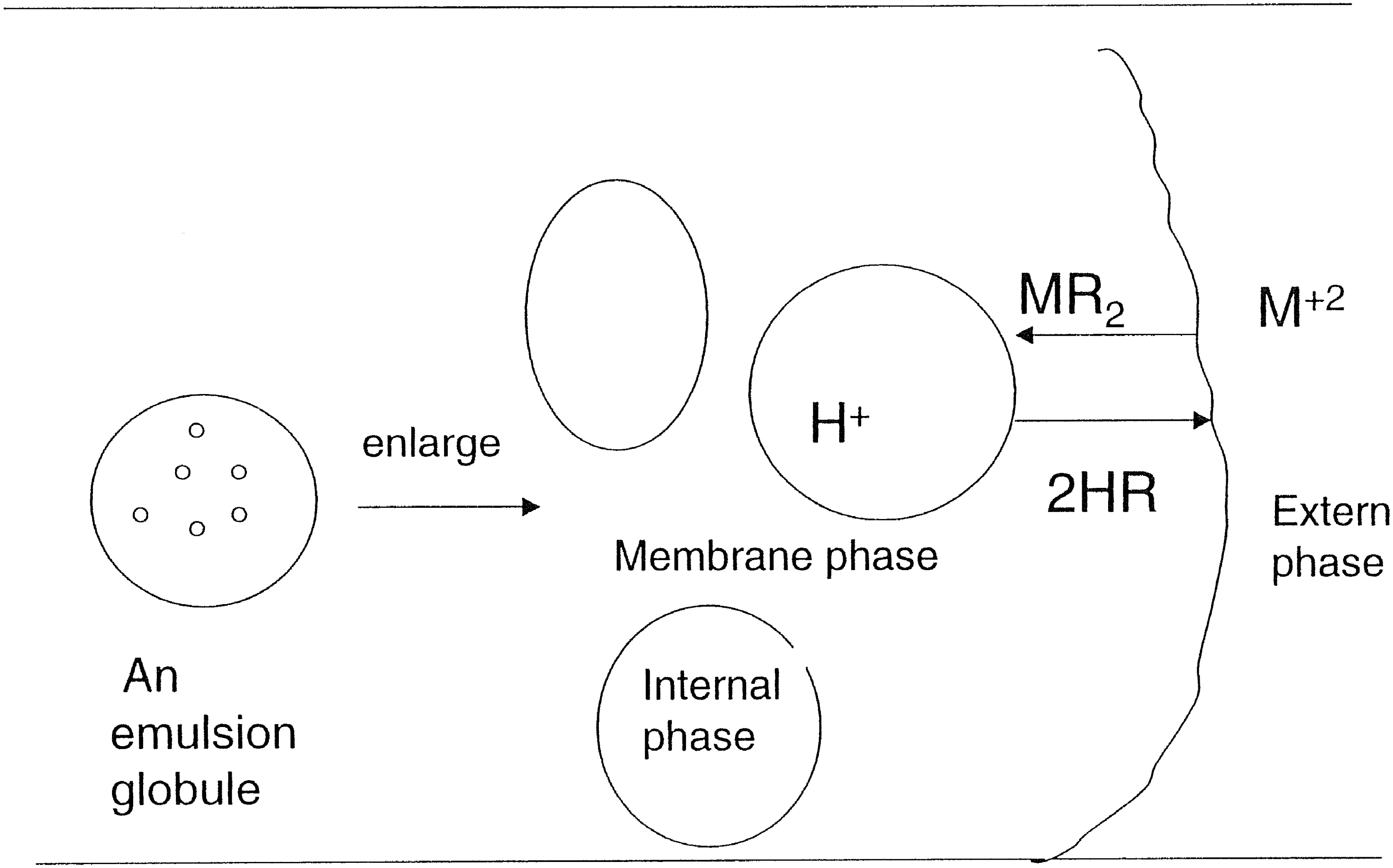

Figure 1.3 Mechanism of Mass Transport of ELM System

The mechanism involves the following steps

1. Mass transfer of copper ion from external bulk phase through mass transfer resistance film to external interface between external phase and membrane phase.

2. Copper ion reacts with the carrier or extractant (HR) of the membrane phase at the interface of external and membrane phase.

$$Cu^{2+}|_{\text{external}} + 2HR \quad CuR_2\,|_{\text{interface (external/membrane)}} + 2H^{+}|_{\text{external}}$$

3. Mass transfer of CuR_2 in the membrane phase from the external /membrane interface to the membrane /internal interface

$$CuR_2|_{\text{interface (external/membrane)}} \quad CuR_2\,|_{\text{interface (membrane/internal)}}$$

4. Membrane-soluble complex (CuR_2) at the membrane/internal interface reacts with hydrogen ions from the internal phase.

$$CuR_2|_{\text{interface (membrane/internal)}} + 2H^{+}|_{\text{internal}} \quad 2HR|_{\text{interface(membrane/internal)}} + Cu^{2+}|_{\text{internal}}$$

The metal ions are released from the membrane phase into the internal phase.

5. Mass transfer of extractant in the membrane phase from the membrane/internal interface to the external/membrane interface.

$$HR|_{\text{interface(membrane/internal)}} \quad HR|_{\text{interface(external/membrane)}}$$

This facilitated transfer of copper ions occurs when the pH value of the internal phase is lower in value than that of the external phase.

1.3 Advantages of Emulsion Liquid Membrane

There are several advantages of the emulsion liquid membrane process over the solvent extraction process. They are: a. Simultaneous extraction and stripping take place in one single step rather than two separate steps as required by solvent extraction. b. The ELM feature of simultaneous extraction and stripping removes the equilibrium limitation inherent in solvent extraction. Therefore, the completed removal of the solute from feed can be achieved with single-step ELM extraction. c. Another advantages resulting from non-equilibrium feature of an ELM process is the significant reduction of the extractant inventory required for the ELM extraction versus solvent extraction. Reduction by a factor of more than 10 is possible so that an expensive extractant can be used. d. High fluxes are possible. By combining the advantages of a high diffusion coefficient in the liquid with the added carrying capacity of the carrier, a larger flux than that of a polymer membrane is possible. e. Very selective separations are possible. The selectivity nature of the carrier provides much better separation than those obtained based solely on relative solubility and diffusion. f. Ions can be concentrated. Coupled transport allows one to pump ions against their concentration gradient. g. ELM is reported up to 40% less expensive than solvent extraction (47).

1.4 Theoretical Modeling of ELM Systems

Emulsion Liquid Membrane systems are a novel and effective way to recover metal ions from wastewater. In the past three decades, the separation of a variety of metals by ELM has been studied by many investigators. For each indvidual metal, to find the best experimental conditions, one must change one experimental condition, while fixing the other conditions. Then one changes another condition and fixes the remaining conditons. This process continues until the best conditions are found for every parameter. For example, it is desired to extract copper with LIX-64 as carrier in the membrane phase and sulfuric acid in the internal phase. First, if one wants to know the best volume percentage for the carrier, one must fix the other parameter and change the carrier volume from 3%, 5%, 7%, 10%, 20%.... Then if one wants to know the best pH value for the external phase, one must fix the other parameter and change pH from 1, 2, 3, 4, 5...

The successful recovery of one metal requires a great amount of tedious experimental work. It can be very frustrating at times, for even after several trials under every condition, it still may not be able to achieve the desired recovery rate.

This thesis is going to present the mathematical models to provide theoretical guidance to optimal recovery conditions and to predict maximum achievable efficiencies for metal recovery from wastewater.

Much research has been done on wastewaster treatment with the ELM systems. However, few researchers have focused on the mathematical modeling of the system. Ho and coworkers developed a model for type 1 facilitation in 1982 which is not going to be studied in this thesis(48). Lorbach and Marr developed a model for type 2 in 1987(5). Lorbach and Marr's model took into account the diffusion of carrier and carrier-solute complex in the membrane globules and the reversible reactions at the external and internal interfaces. Although some simplifications have been made on constant summation of free and complex carrier, constant pH in the external phase and eliminated resistance for the peripheral thin membrane layer based on Teramota and Kataoka's model (49, 50), there were still four parameters dealing with extraction and stripping equilibrium that are quite difficult to determine correctly.

Currently, Sang Cheol Lee and coworkers developed a general physical model of a typical batch extraction system employing an emulsion liquid membrane process for the extraction of silver (51). It is a very good model. However, it made a simplification that the mass transfer resistances of silver and hydrogen ions in the external aqueous phase were neglected. It is shown in Wang's thesis (1984) that the external phase resistances can not be neglected (52). Sang et al did not produce analytical solutions for their model. Instead they solved their model with computer similation. This study will not neglect the external phase resistence and will give analytical solutions to our mathematical model.

It is interesting to know that Rajdip and coworkers (1997) developed a new model of batch-extraction in ELM considering interaction of globules for type one facilitation (53). Jae Hwa Chang and coworker (1992) had a model for enzymatic reaction with ELM (54).

In this thesis, based on the previous work of C. R. Huang's group (29, 52), theoretical models of the extraction and stripping distribution coefficients and theroretical models of the chemical reactions and transport phenomena in the internal phase will be made. The theoretical predictions and experimental results will be compared.

CHAPTER 2

MATHEMATICAL MODELING OF TRANSPORT PHENOMENA IN ELM SYSTEMS

2.1 Constructing Mass Transport Model of ELM Systems

2.1.1 Introduction

Figure 2.1 shows the mass transport operation that will be modeled. The model describes diffusion of the solute in the external phase, mass transfer of the solute across the film between the external phase and membrane phase, chemical equilibrium of the extraction reaction on the external-membrane interface, simultaneous diffusion of solute-carrier complex inside the globule membrane phase, and chemical equilibrium of the stripping reaction on the membrane-internal interface. Simultaneous partial differential equations were solved analytically by the Laplace transform method. Some dimensionless groups are found with special physical meanings to characterize the emulsion liquid membrane system. The analytical solutions of the model give concentration profiles of solute in the external phase $C_e(t)$, concentration profile of the metal-carrier complex in the membrane phase $C_m(r, t)$ and surface concentration of solute on the external membrane interface. The extraction and stripping reactions are assumed to be very fast so that they are not the rate limiting step and chemical reaction equilibrium has been reached at interfaces (52). This assumption is made because of the physical structure of the ELMs. The radius of the internal droplet of ELM is 1-10 μm. The radius of the emulsion globule is 0.1-0.2 mm. Such small droplets create huge surface areas for two phase contact so that extraction and stripping reactions are assumed to reach equilibrium even though the reaction kinetics are not too fast. Actually, most of the extraction and stripping reactions

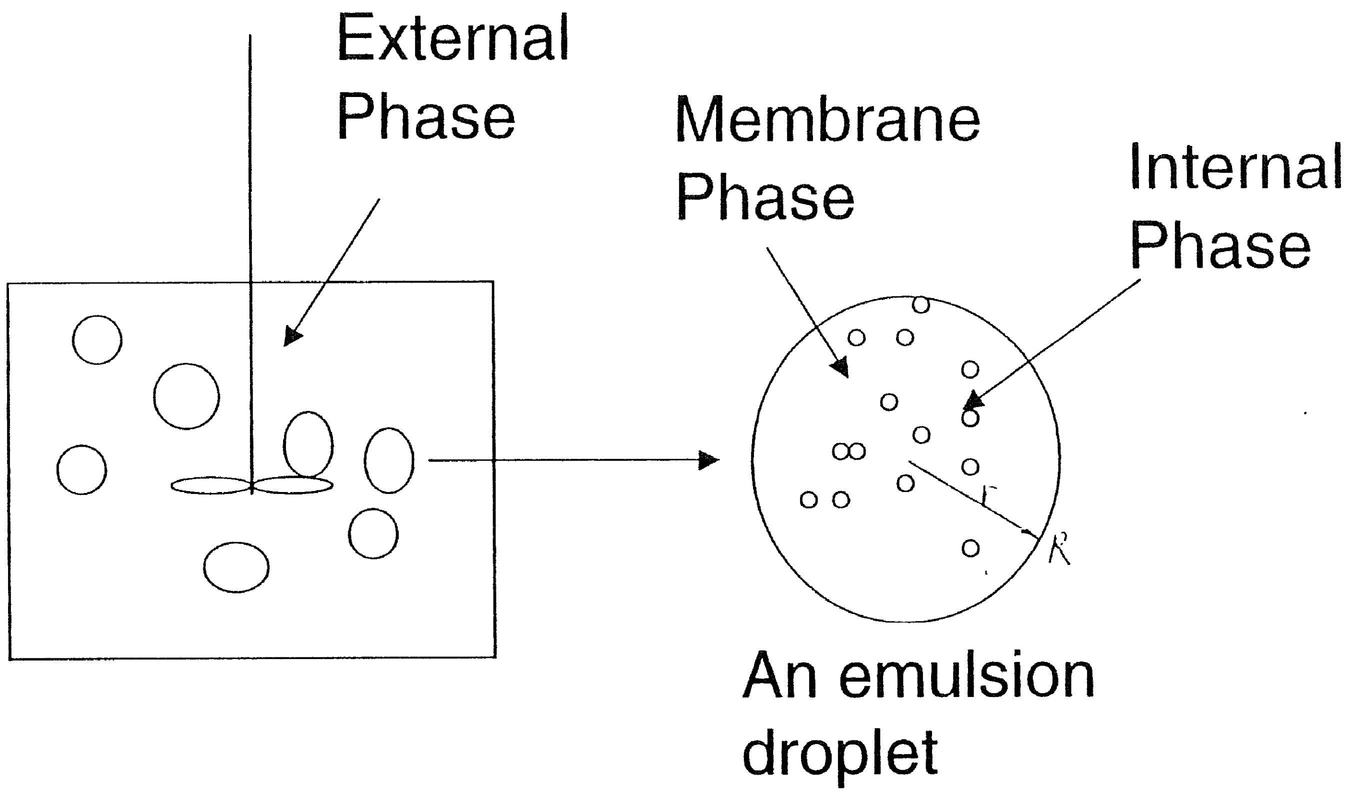

Figure 2.1 Figure Used for Mathematical Modeling

are very fast because they are ion-exchange reactions. Other simplifications have been made in order to describe the complicated ELMs (52, 29): a. Emulsion globule is monodisperse and spherical. Saunter mean radius is good enough to describe the globule size (49, 55). b. There is no internal circulation inside the globule, due to sufficient use of surfactant (56,57). Thus, mass transfer in the membrane phase is by diffusion only and the effective diffusivity is constant in the membrane phase. c. There is no coalescence and redipersion of emulsion globules (58). d. No volume change for each phase. e. The internal mass transfer resistance is negligible since it is so small in size. f. The tank is well mixed so that the concentration in the external phase is uniform. g. Leakage from the internal phase into the external phase is negligible.

Based on the above assumptions, a mathematical model of transport phenomena in ELM systems has been developed.

2.1.2 Mass Transport Model of ELM

First, it is assumed that the solute used is a typical metal ion M^{+2}. Following the work of K. C. Wang (1984) and D.W. Zhou (1996), the mass transport model from the external phase to internal is established (52, 29).

1. ***External phase mass transfer resistance from external phase to the external-membrane interface.***

There is resistance for diffusion from the external phase to external-membrane interface. Wang (1984) proved that this resistance could not be neglected.

$$V_e \frac{dC_e}{dt} = -N(4\pi R^2)k(C_e - C_e^*) \tag{2.1}$$

Initial Condition: $C_e = C_{e0}$, when $t = 0$

where $C_e(t)$= Concentration of M^{+2} in the external phase(mol/l)

$C_e^*(t)$=Concentration of M^{+2} in the external phase at the external-membrane interface(mol/l)

C_{e0}= initial concentration of M^{+2} in the external phase(mol/l)

k= external mass transfer coefficient(m^2/sec)

V_e= volume of external phase (ml)

N = total number of emulsion droplets

R = radius of a emulsion droplet (m)

2. *Mass fluxes at the external-membrane interface*

At the interface of the external-membrane, there is no solute accumulation. Thus, the flux of mass transfer outside the external-membrane interface is equal to the flux of mass diffusion inside the external- membrane interface. The concentration of solute in external phase, C_e, is greater than that on external-membrane interface, C_e^*. The difference of these two concentrations is the driving force to overcome external film resistance.

$$N(4\pi R^2)k(C_e - C_e^*) = N(4\pi R^2)D_e(\frac{\partial C_m}{\partial r})_{r=R} \qquad (2.2)$$

where $C_e^*(t)$ = Concentration of M^{+2} in the external phase at the external-membrane interface(mol/l)

$C_m(r, t)$ = Concentration of M^{+2} (in the form of metal-extractant complex) in the membrane phase(mol/l)

D_e = effective diffusivity of solute-carrier complex in emulsion phase (m^2/sec)

$k(C_e - C_e^*)$ = the flux of mass transfer outside external-membrane interface and

$D_e(\frac{\partial C_m}{\partial r})_{r=R}$ = the flux of mass diffusion inside external membrane interface.

3. ***Equilibrium at the external-membrane interface***

Since chemical reaction at the external-membrane interface reaches equilibrium, therefore:

$$C_{me}^{*} = pC_{e}^{*} \tag{2.3}$$

where p = extraction distribution coefficient

C_{me}^{*} = the concentration of the metal-extractant complex in the membrane phase at the external-membrane interface (or at r = R) (mol/l)

Equation (2.3) shows that the larger the extraction distribtuion coefficient, p, is the better the performance

4. ***Mass transfer inside a droplet of membrane phase***

$$V_m \frac{\partial C_m}{\partial t} = (V_m + V_i) D_e \frac{1}{r^2} \frac{\partial}{\partial r}\left(r^2 \frac{\partial C_m}{\partial r}\right) - V_i \frac{\partial C_i}{\partial t} \tag{2.4}$$

at t =0, C_m=0, at all r

C_m=finite, when r = 0; C_m= C_{me}^{*}, when r = R

Where C_i(r, t)= Concentration of solute in internal phase of a droplet (mol/l)

V_m = volume of membrane phase (ml)

V_i = volume of internal phase (ml)

V_m+ V_i = total volume of emulsion (ml)

Note: there is no internal mass transfer film being considered

5. ***Equilibrium at internal-membrane interface***

Wang (1984) proved that the internal mass transfer film is negligible. Therefore, in this thesis, there is no internal mass transfer film being considered. Thus, the solute concentration in the internal phase is the same as the solute concentration at the internal-membrane interface. Since at the internal-membrane interface, the chemical reaction reaches equilibrium, therefore:

$$C_i^* = C_i = qC_{mi}^* = qC_m \tag{2.5}$$

C_i=0, when t=0 for all r

where C_i^*=concentration of solute in the internal phase of the membrane-internal interface(mol/l)

C_{mi}^* = concentration of solute in the membrane phase of membrane-internal Interface (mol/l)

q = stripping distribution coefficient

Equation (2.5) shows that the larger the stripping distribution coefficient, q, is, the better the performance.

6. Recovery Efficiency E

The recovery efficiency is defined as:

$$E(t) = 1 - \frac{C_e(t)}{C_{e0}} \tag{2.6}$$

2.2 Analytical Solutions

The above four partial differential equations, together with two equilibrium equations are all linear. Laplace transform method is applied to derive the concentration profiles of $C_e(t)$, $C_e^*(t)$ and $C_m(r, t)$.

Combining equations (2.4) and (2.5), gives:

$$\frac{(V_m + qV_i)}{(V_m + V_i)} \frac{\partial C_m}{\partial t} = D_e \frac{1}{r^2} \frac{\partial}{\partial r}(r^2 \frac{\partial C_m}{\partial r}) \tag{2.7}$$

Equation 2.7 shows that concentration of complex in membrane phase C_m is proportional to concentration of solute in internal phase C_i , so that these two variables can be simply combined into one. Physically it means that the internal droplets are so small that there is no concentration difference inside the droplet and the complex is quickly stripped as soon as it reaches the internal interface.

The procedure for solving these equations

1. *Convert equations to dimensionless form*

Let $$U_e = \frac{C_e}{C_{e0}} \tag{2.8}$$

$$U_m = \frac{C_m}{pC_{e0}} \tag{2.9}$$

$$U_e^* = \frac{C_e^*}{C_{e0}} \tag{2.10}$$

$$U_m^* = \frac{C_m^*}{C_{e0}} \tag{2.11}$$

$$K_0 = \frac{Rkf}{D_e} \tag{2.12}$$

$$\frac{\tau}{\omega} = \frac{D_e t}{\omega R^2} \tag{2.13}$$

$$= \frac{r}{R} \tag{2.14}$$

Equations 2.1 to 2.5 and equation 2.7 are converted into dimensionless form:

External: $\frac{dU_e}{\partial \tau} = -K_0(U_e - U_e^*)$ (2.15)

$$G(\frac{\partial U_m}{\partial \nu})|_{\nu=1} = (U_e - U_e^*) \quad (2.16)$$

Equilibrium: $U_e^* = U_m^*$ (2.17)

Initial condition: $U_e = U_e^* = 1$ when $\tau = 0$ (2.18)

Membrane: $\omega \frac{\partial U_m}{\partial \tau} = \frac{1}{\nu^2}\frac{\partial}{\partial \nu}(\nu^2 \frac{\partial C_m}{\partial \nu})$ (2.19)

Initial conditions: $U_m = 0,$ when $\tau = 0$ (2.20)

Boundary conditions: $U_m = \mathit{finite}$ when $\nu = 0$ (2.21)

$U_m = U_e^*$ when $\nu = 1$ (2.22

2. *Solve equation(2.19) by the Laplace Transform method and obtain* $U_m = f(\nu, \tau)$

$$U_m = \frac{C_m}{pC_{e0}} = \frac{3}{B+3} + \sum_{n=1}^{\infty} \frac{2(B - Gb_n^2)(\frac{\sin(b_n * \nu)}{\nu * \sin(b_n)})}{3B + B^2 + b_n^2 + Gb_n^2(Gb_n^2 - 2B - 1)} \exp(-\frac{b_n^2}{w}\tau) \quad (2.23)$$

3. *Use equation (2.16) and equation (2.23) to find* $(U_e - U_e^*)$ *which is a function of* τ *only*

4. *Use Equation (2.15) to find* $U_e(\tau)$

$$U_e = \frac{C_e}{C_{e0}} = \frac{3}{B+3} + \sum_{n=1}^{\infty} \frac{2B}{3B + B^2 + b_n^2 + Gb_n^2(Gb_n^2 - 2B - 1)} \exp(-\frac{b_n^2}{\omega}\tau) \quad (2.24)$$

5. ***Find $U_e^* = U_e\big|_{r=R}$, the concentration of metal-extractant complex at external-membrane interface***

$$U_e^* = \frac{C_e^*}{C_{e0}} = \frac{3}{B+3} + \sum_{n=1}^{\infty} \frac{2(B - Gb_n^2)}{3B + B^2 + b_n^2 + Gb_n^2(Gb_n^2 - 2B - 1)} \exp(-\frac{b_n^2}{w}\tau) \qquad (2.25)$$

The concentration profiles for the external phase, the external-membrane interface and the membrane phase are respectively:

$$\frac{C_e}{C_{e0}} = \frac{3}{B+3} + \sum_{n=1}^{\infty} \frac{2B}{3B + B^2 + b_n^2 + Gb_n^2(Gb_n^2 - 2B - 1)} \exp(-\frac{b_n^2}{\omega}\tau) \qquad (2.24)$$

$$\frac{C_e^*}{C_{e0}} = \frac{3}{B+3} + \sum_{n=1}^{\infty} \frac{2(B - Gb_n^2)}{3B + B^2 + b_n^2 + Gb_n^2(Gb_n^2 - 2B - 1)} \exp(-\frac{b_n^2}{\omega}\tau) \qquad (2.25)$$

$$\frac{C_m}{pC_{e0}} = \frac{3}{B+3} + \sum_{n=1}^{\infty} \frac{2(B - Gb_n^2)(\frac{\sin(b_n * v)}{v * \sin(b_n)})}{3B + B^2 + b_n^2 + Gb_n^2(Gb_n^2 - 2B - 1)} \exp(-\frac{b_n^2}{\omega}\tau) \qquad (2.23)$$

Where

b_n are eigenvalues of the equation

$$\tan(b_n) = \frac{b_n(B - Gb_n^2)}{B + b_n^2(1 - G)}, n \geq 1 \qquad (2.26)$$

$$G = \frac{pD_e}{Rk} \qquad (2.27)$$

$$B = pf'\omega \qquad (2.28)$$

$$f' = \frac{V_i + V_m}{V_i + V_m + V_e} \qquad (2.29)$$

$$e = \frac{V_i}{V_i + V_m} \qquad (2.30)$$

$$\omega = 1 - e + eq \qquad (2.31)$$

Mathematical details can be found in the appendix of D.W. Zhou's thesis (29).

As time approaches infinity, equation (2.24) becomes:

$$\frac{C_e}{C_{e0}} = \frac{3}{B+3} \tag{2.32}$$

At equilibrium, recovery efficiency $E(\infty) = 1 - \frac{C_{e\infty}}{C_{e0}} = \frac{B}{B+3}$ (2.33)

Equation (2.32) means that when the system reaches equilibrium, the external concentration is 3/(B+3). The parameter B can be defined as the emulsion capacity of the system. Equation (2.28) to Equation (2.30) give the expression of B value as a function of extraction distribution coefficient, stripping distribution coefficient, volume ratio of emulsion phase to total volume and volume ratio of internal phase to emulsion phase. The larger the B value is, the bigger the recovery efficiency. Thus any effort to increase the B value will optimize the ELM system.

2.3 Discussion of Analytical Solution

2.3.1 Eigenvalues b_n

The term RHS(b_n) is used to denote the functional dependence of the right hand side of the eigenvalue equation (2.26). Hence,

$$RHS(b_n) = \frac{b_n\left(B - Gb_n^2\right)}{B + b_n^2(1-G)} \tag{2.34}$$

RHS(b_n) depends on the parameters B and G. As shown in Figures 2.2(a) and 2.2(b), RHS(b_n) behaves very differently depending on whether G is greater or smaller than 1.

If 0<G<1 (Figure 2.2(a)), the function RHS(b_n) first increases from 0 to a maximum positive number, then decreases toward negative infinity as b_n approaches infinity.

If G>1 (Figure 2.2(b)), the function RHS(b_n) has a singularity at

$$b_n = b_s = \sqrt{\frac{B}{G-1}} \tag{2.35}$$

The singular point b_s divides the entire positive b_n regime into two sub-regimes. For 0< b_n < b_s, RHS(b_n) first increases from 0 to a maximum positive number, then decreases toward negative infinity as b_n approaches b_s. For b_n > b_s, RHS(b_n) first decreases from positive infinity to a minimum positive number, then increases to positive infinity as b_n approaches infinity.

The left hand side of the equation 2.26, LHS(b_n)=tan(b_n), divides the entire positive b_n regime into an infinite number of sub-regimes spanning between (n-1/2)π and (n+1/2)π, n=1,2,3,…, plus a sub-regime between 0 and π/2. There is no eigenvalue in the sub-regime between 0 and π/2.

For G<1, each sub-regime between (n-1/2)π and (n+1/2)π contains one eigenvalue. As n approaches infinity, the right-hand-side RHS(b_n) approaches negative infinity. For large value of n, the nth eigenvalue therefore approaches (n-1/2) π.

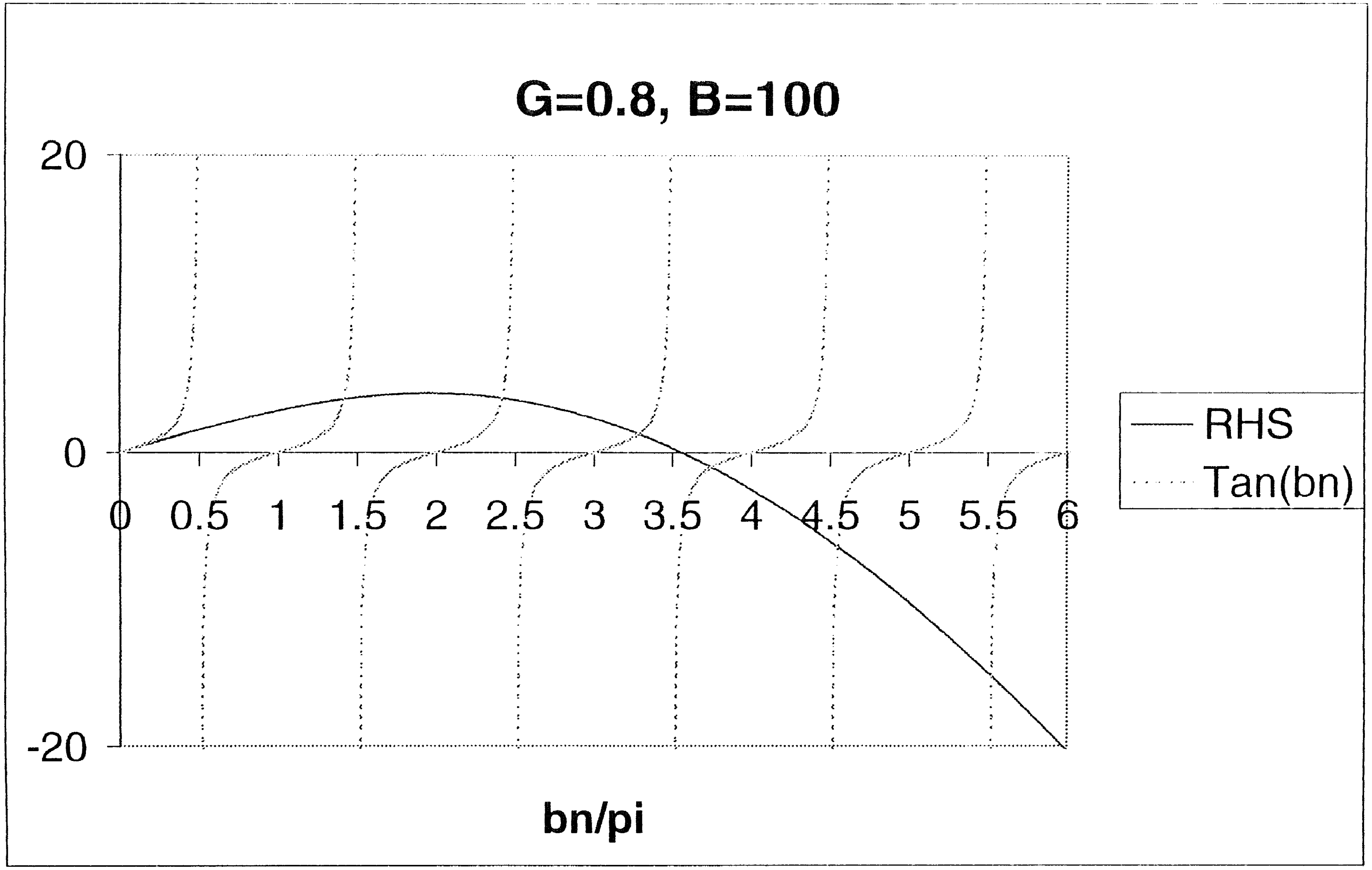

Figure 2.2a Determination of Eigenvalue when G<1

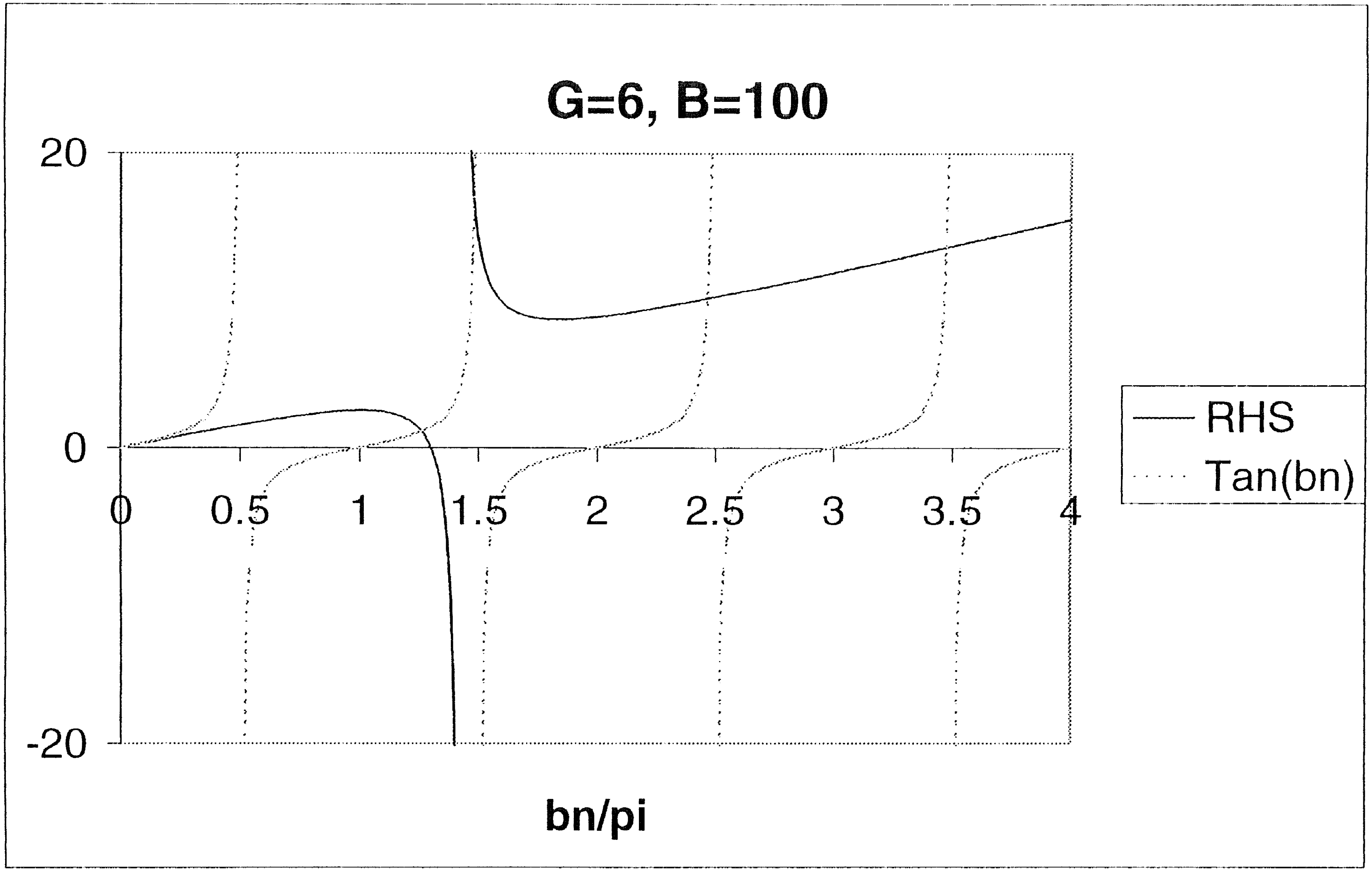

Figure 2.2b Determination of Eigenvalue when G>1

For G>1, each sub-regime between (n-1/2)π and (n+1/2)π contains one eigenvalue, except the sub-regime enclosing the singular point b_s of the function RHS(b_n), which contains two eigenvalues. As n approaches infinity, the right-hand-side RHS(b_n) approaches positive infinity. For large values of n, the nth eigenvalue therefore approaches (n+1/2) π.

Previous work failed to take note of the singular behavior in the G>1 case. As a result, one term was missing in the expressions of the concentration profiles for finite times. In some cases, this term corresponds to one of the very first (smallest) eigenvalues, and can contribute significantly to the time dependent concentration profile. However, this effect has no impact on the equilibrium concentrations for infinite time. In 2.3.2, the importance of correctly handling the singularity in the G>1 case is illustrated.

2.3.2 Impact of Singularity on Concentration Profile

For the G=6, B=100 case, as an example, the impact of the singularity on the external phase concentration profile

$$U_e = \frac{C_e}{C_{e0}} \tag{2.8}$$

and the external-membrane interface concentration profile

$$U_e^* = \frac{C_e^*}{C_{e0}} \tag{2.10}$$

is illustrated.

The singularity in the function RHS(b_n) is located at

$$b_s = \sqrt{\frac{B}{G-1}} = \sqrt{\frac{100}{6-1}} \approx 4.47 \approx 1.42\pi$$

u_n is used to denote the contribution to the initial normalized external phase concentration $U_e(t=0)=1$ from the term associated with the nth eigenvalue b_n, the following table shows the first few eigenvalues as multiples of π and their contributions u_n.

Table 2.1 Eigenvalues and their contributions to initial external concentration

n	1	2	3	4	5	6	7
b_n/π	1.26	1.48	2.47	3.48	4.48	5.48	6.49
u_n	0.78296	0.18411	0.00294	0.00053	0.00017	0.00007	0.00003

The second eigenvalue can be found only by correctly handling the singularity. Note the contribution from the term associated with this eigenvalue is over 18%. Figure 2.3 compares the external phase concentration profiles obtained in two different approaches, by considering the singularity effect (this study) and by neglecting the singularity effect (previous work). As expected, the external phase concentrations converge as time approaches infinity, but differ significantly initially. Neglecting the singularity effect, therefore, leads to the incorrect initial normalized concentration value of 0.816, which is significantly less than the correct value of 1.

The parameter u_n^* is used to denote the contribution to the initial normalized external-membrane interface concentration $U_e^*(t=0)=0$ from the term associated with the

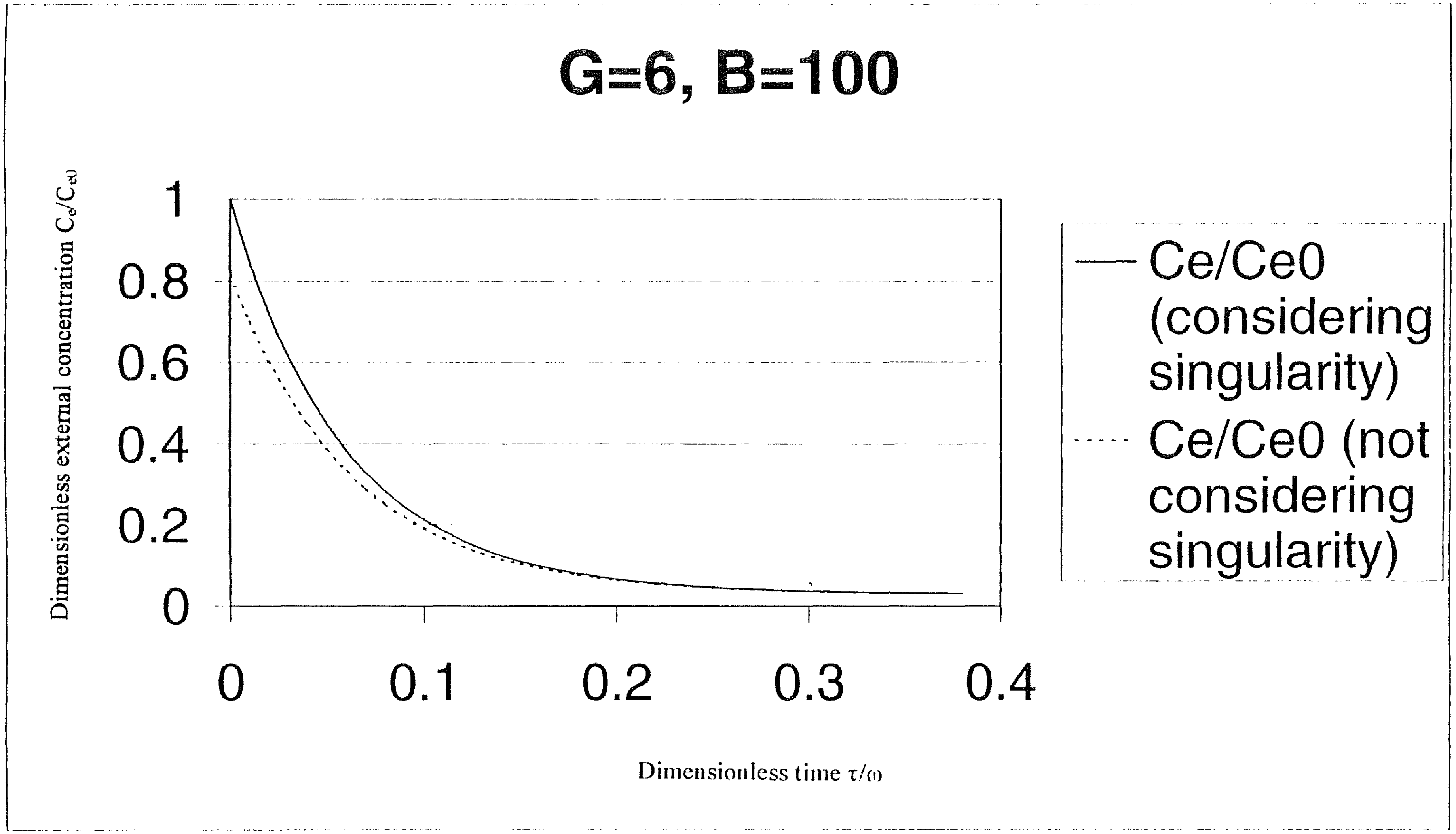

Figure 2.3 Dimensionless External Concentration Profiles Considering and Not Considering Singularity of Eigenfunction

nth eigenvalue b_n, the following table shows the first few eigenvalues as multiples of π and their contributions u_n^*.

Table 2.2 Eigenvalues and their contributions to initial external-membrane interface concentration

n	1	2	3	4	5	6	7
b_n/π	1.26	1.48	2.47	3.48	4.48	5.48	6.49
u_n^*	0.04560	-0.05507	-0.00767	-0.00325	-0.00184	-0.00119	-0.00084

The second eigenvalue can be found only by correctly handling the singularity. Note the contribution from this eigenvalue is greater in magnitude than that from any other eigenvalues.

Figure 2.4 compares the external-membrane interface concentration profiles obtained in two different approaches, by considering the singularity effect (this study) and by neglecting the singularity effect (previous work). As expected, the exernal membrane interface concentrations converge as time approaches infinity, but differ significantly initially. Especially, neglecting the singularity effect leads to the incorrect initial normalized concentration value of 0.05507, which differs significantly from the correct value of 0.

2.3.3 Concentration Profile at External-membrane Interface

Figure 2.4(a) shows the concentration profile at the external-membrane interface for G=10 and B=100. Figure 2.4(b) shows the concentration profile at the external-membrane interface for G=0.8 and B=100. In both cases, the concentration starts from 0 at time 0 and eventually approaches the equilibrium value B/(B+3) = 0.29 as time goes to

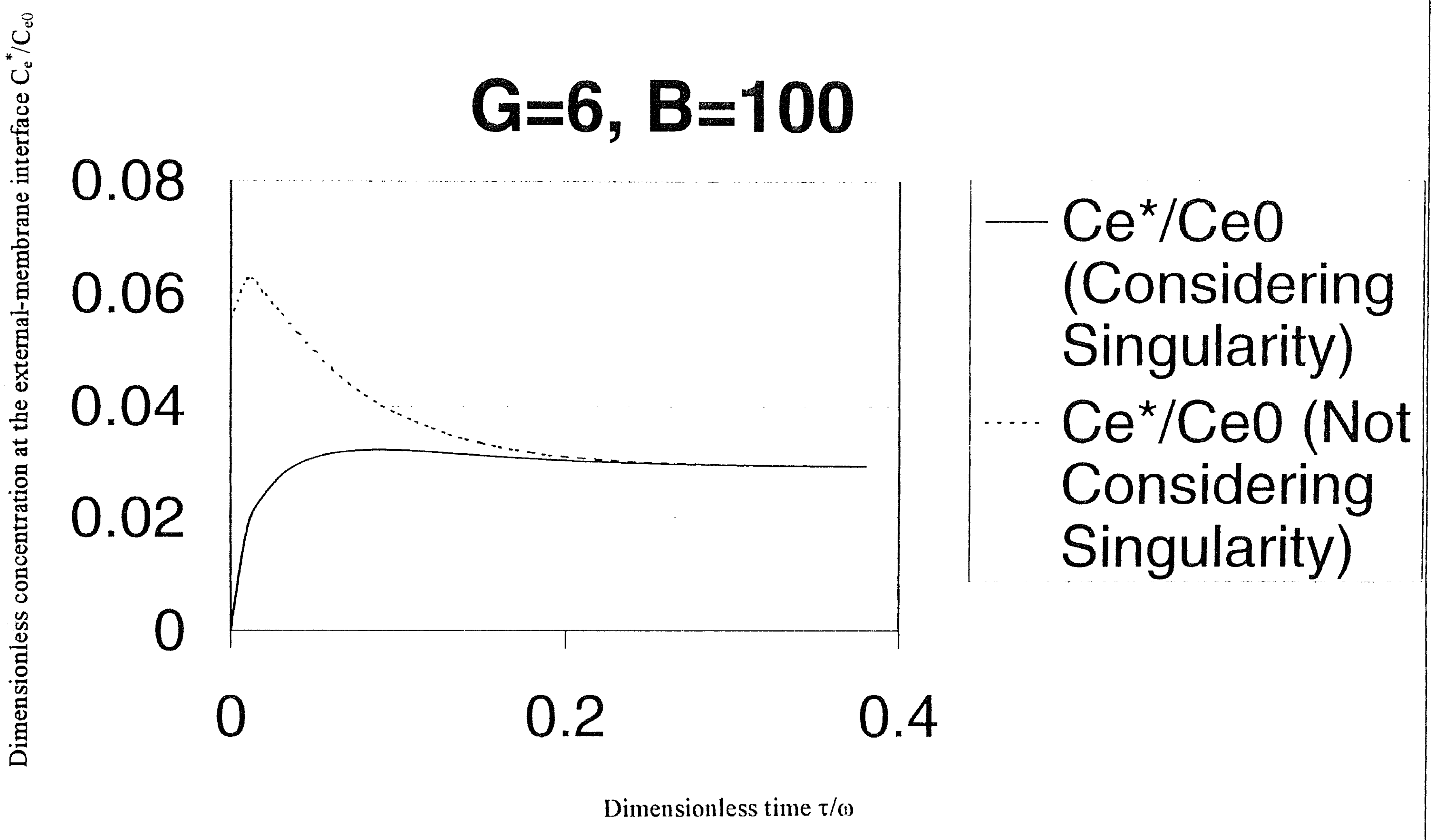

Figure 2.4 Dimensionless Concentration Profiles at the External-membrane Interface Considering and not Considering Singularity of Eigenfunction

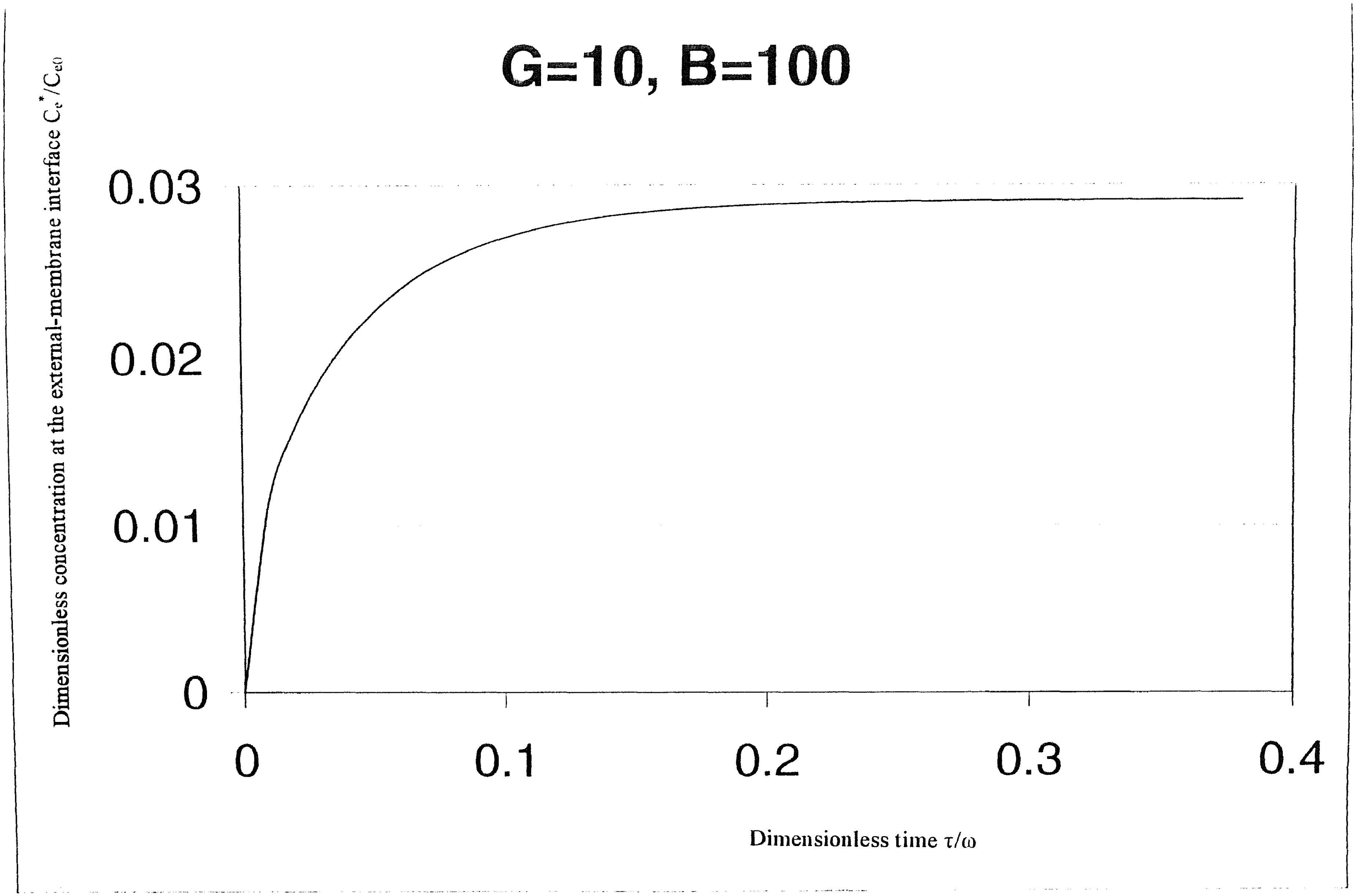

Figure 2.4a Dimensionless Concentration Profile at the External-membrane Interface with a Larger G Value

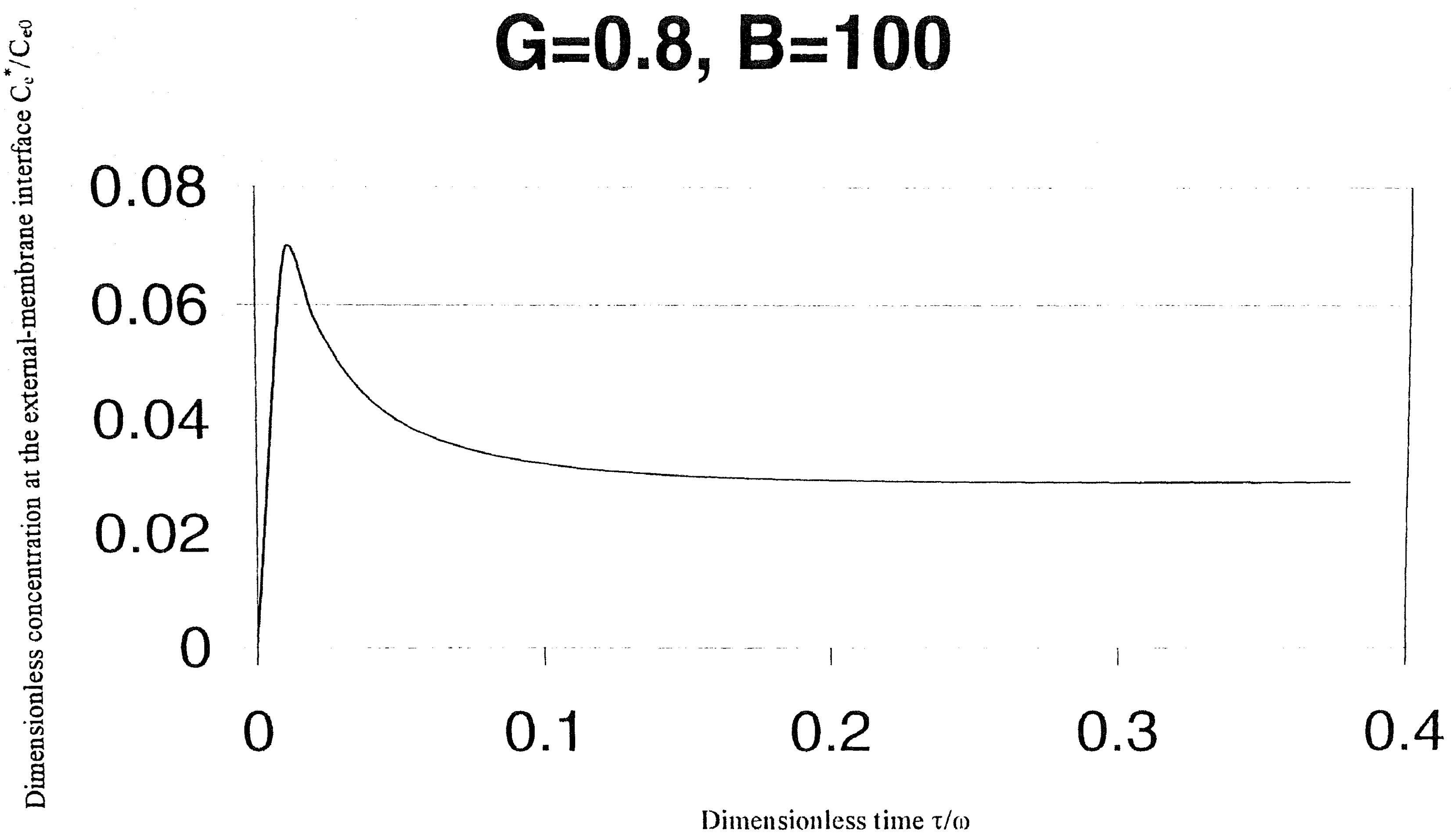

Figure 2.4b Dimensionless Concentration Profile at the External-Membrane Interface with a Smaller G Value

infinity. However, for large value of G (Figure 2.4(a)), the external-membrane interface concentration increases monotonically from 0 to the equilibrium value, while for small value of G (Figure 2.4(b)), the external-membrane interface concentration first rises above the equilibrium value before decreasing monotonically to the equilibrium value. To understand such behavior, recall that G is the ratio of the external film resistance to the emulsion diffusion resistance, as defined in Equation (2.27). Larger values of G mean smaller emulsion diffusion resistances and, hence, faster mass transfer rates in the emulsion. For large volumes of G, metal ions arriving at the external-membrane interface diffuse quickly into the internal phase without causing any accumulation at the interface (Figure 2.4(a)).

For small values of G, initially metal ions arrive at the external-membrane interface at a rate greater than can be transferred into the internal phase causing an accumulation at the interface. Eventually the accumulation diminishes as fewer metal ions arrive at the external-membrane interface from the external phase. The external-membrane interface concentration gradually decreases to its equilibrium value (Figure 2.4(b)).

CHAPTER 3

MATHEMATICAL MODELING OF CHEMICAL REACTIONS IN ELM SYSTEMS

3.1 Literature Review

Professor Ching-Rong Huang's group has worked on mass transfer mathematical modeling of the ELM system since the early 1980's. This model is the most complete one in all the published models describing ELM systems. It considers diffusion in the external phase, external film resistance, diffusion in the membrane phase and chemical equilibrium at the two interfaces. This model is the only one that gives analytical solutions.

K. C. Wang (1984) first established a mass transfer model of ELM under the guidance of Dr. Ching-Rong Huang. He built a solid foundation for later researchers in this area. However, he did not study the extraction and stripping distribution coefficients. The two coefficients are simply input parameters to the model (52).

D. W. Zhou (1996) applied a mass transport model to arsenic (As) and strontium (Sr) extraction experiments. He also modified Wang's model to consider leakage phenomena in the ELM system. However, he did not do research in the extraction and stripping distribution coefficients. Extraction and stripping distribution coefficients were considered as constants to be determined by fitting experimental data (29).

Previous studies did not model the chemical reactions at the interfaces that determine extraction and stripping distribution coefficients. Chemical reactions in the internal phase were also neglected.

In this thesis, extraction and stripping coefficients will be studied. A theoretical model of extraction and stripping distribution coefficients will be given. The chemical reaction in the internal phase and its impact to the mathematical models of ELM system will be theoretically modeled. The existing models will be modified considering the internal phase chemical reactions. In the next chapter theoretical predictions will be compared with experimental results.

3.2 Equilibrium Constants of Chemical Reactions

The chemical reactions in the emulsion liquid membrane system are interfacial reactions, which are different from reactions in the same phase. (When an equation for a chemical reaction is written, a subscript should be used to identify each reactant and each product with respect to their phases.) These interfacial reactions introduce complexities in studying the equilibrium constant, which is needed to determine the extraction distribution coefficient and stripping distribution coefficient.

For the reaction:

$$aA + bB \Leftrightarrow cC + dD \tag{3.1}$$

and the definition of equilibrium constant, at low pressure, the following equation results(59):

$$K_a = \frac{\gamma_C^c [C]^c \gamma_D^d [D]^d}{\gamma_A^a [A]^a \gamma_B^b [B]^b} = K_\gamma K_x \tag{3.2}$$

Henry's law is used to the definition of activity coefficient here:

$$\gamma_i = \frac{\hat{f}_i}{f_i^0 [i]} \tag{3.3}$$

Where A, B, C, D = the components for the reaction involved

a, b, c, d = molar stoichiometric coefficients

γ_i = the activity coefficient of component i

[ ] identifies the concentration of the reactants and products at equilibrium.

$\hat{f}_i$ = the fugacity of a component i in a mixture

$f_i^{\,0}$ = the fugacity of pure component i at standard state (Henry's law)

$$K_\gamma = \frac{\gamma_C^c \gamma_D^d}{\gamma_A^a \gamma_B^b}$$

For the ELM system, a typical metal (M^{2+}) complexion with LIX extractant (RH) is described by

$$M^{2+}(e) + 2RH(m) \Leftrightarrow MR_2(m) + 2H^+(e) \tag{3.4}$$

where e identifies the external phase

m identifies the membrane phase

First, assume that the equilibrium constant of above reaction can be written as follows:

$$K = \frac{\{MR_2\}_m \{H^+\}_e^2}{\{M^{2+}\}_e \{RH\}_m^2} \tag{3.5}$$

Metal complexion with n dimers of extractant D2EHPA [$(RH)_2$] is described by

$$M^{2+}(e) + n(RH)_2(m) \Leftrightarrow MR_2(m) + 2H^+(e) \tag{3.6}$$

and

$$K = \frac{\{MR_2\}_m \{H^+\}_e^2}{\{M^{2+}\}_e \{RH\}_m^n} \tag{3.7}$$

Where: {} represents activities that are products of concentrations and activity coefficients (60).

There are many models to calculate the activity coefficients for Non-electrolyte and electrolyte solutions. The aqueous phase of ELM system is an electrolyte solution. The organic phase of the ELM system is a non-electrolyte solution.

The theory proposed in 1923 by Debye and Huckel provides a rigorous anchor point for most engineering models of electrolyte solutions (59). The form of the Debye-Huckel limiting law is:

$$\log_{10}\gamma_i = \frac{1.8248*10^6\rho_s^{1/2}}{(D_sT)^{3/2}}(z_i^2)I^{1/2} = -Az_i^2I^{1/2} \tag{3.8}$$

where D_s = static dielectric constant of the solvent

ρ_s = the density of the solvent

z_i = electrical charge or valance

I = the ionic strength of solution

$$I = \frac{1}{2}\sum_{i=1}^{n} c_i z_i^2 \tag{3.9}$$

c_i = the concentration of ionic species

If the solvent is water at 25 °C, D_s=78.54, ρ_s=1.0Kg/L, and A=0.510, then:

$$\log_{10}\gamma_i(25^\circ C, aqueous) = -0.510z_i^2I^{1/2} \tag{3.10}$$

The Extended Debye-Huckel form can produce more accurate results,

$$\log_{10}\gamma_i = \frac{-Az_i^2I^{1/2}}{1+Br_0I^{1/2}} \tag{3.11}$$

where r_0 = ionic radius, ranging from 2 to $6*10^{-10}$m

For water at 25 °C, $A=0.510(L/mol)^{1/2}$, $B= 3.2865*10^9\, m^{-1}\, (L/mol)^{1/2}$, $r_0=3.5*10^{-10}$ m, then:

$$\log_{10}\gamma_i(25^{\circ}C, aqueous) = \frac{-0.510 z_i^2 I^{1/2}}{1+I^{1/2}} \qquad (3.12)$$

This equation gives values of γ_i that are too small for many electrolytes. Guggenheim suggested that a linear term, bI, be included in Eq.3.11 and that the b factor be determined by best fit of the data. After examining the values of b for a number of 1:1 and 1:2 electrolytes, Davies (1962) proposed the following equation:

$$\log_{10}\gamma_i = -Az_i^2\left(\frac{I^{1/2}}{1+I^{1/2}} - 0.3I\right) \qquad (3.13)$$

At ionic strengths much above 0.1M, a more accurate representation of experimental data can be obtained if an equation with several adjustable parameters is added to the Guggenheim equation giving:

$$\log_{10}\gamma_i = -Az_i^2 \frac{I^{1/2}}{1+I^{1/2}} + bI + cI^2 + dI^3 \qquad (3.14)$$

the coefficients, b, c, d,..., must be determined experimentally to provide the best-fit approximation of activity coefficients for the system in which they are used (61).

The Pitzer ion interaction model is given by the equation (59):

$$\ln\gamma_i = z_i^2 f^{\gamma} + m\left(\frac{2\nu_+\nu_-}{\nu}\right)B_{\pm}^{\gamma} + m^2\left(\frac{2(\nu_+\nu_-)^{\frac{3}{2}}}{\nu}\right)C_i^{\gamma} \qquad (3.15)$$

Where:

$$f^{\gamma} = -3A_{\phi}\left[\frac{I^{\frac{1}{2}}}{1+bI^{\frac{1}{2}}}\right] + \frac{2}{b}\ln(1+bI^{\frac{1}{2}}$$

$$B_{\pm}^{\gamma} = 2\beta_0 + \frac{2\beta_1}{\alpha^2 I}[1-(1+\alpha I^{\frac{1}{2}} - 0.5\alpha^2 I)\exp(-\alpha^2 I)]$$

$$C_i^{\gamma} = \tfrac{3}{2}C_i^{\phi}$$

The parameters β_0,β_1 and $C_i^{\phi}$are fitted for each ij electrolyte and values for several typical electrolytes can be found in reference. For any 1:1, 1:2, 3:1, 4:1, …, I:1, or 1:j electrolyte, Pitzer recommends setting α to 2.0 and b to 1.2 both in units of $(\text{kg/mol})^{1/2}$. The Pitzer ion interaction model does well in a concentrated electrolyte solution (62). Like many other activity coefficient models of non-ideal behavior of importance to chemical engineering operations, such as the Wilson, NRTL, and UNIQUAC models, the Pitzer ion interaction equations require pure component and binary parameters. The model is more complicated than the Debye-Huckel model, which limits its use in this system.

The following equations define the Meissner model (59):

$$\Gamma_{ij}^{0} = [1+B(1+0.1I)^{q_{ij}^{0}} - B]\Gamma_{ij}^{DH} \qquad (3.16)$$

$$\log_{10}\Gamma_{il}^{DH} = \frac{-0.5107I^{1/2}}{I+CI^{1/2}}$$

$$B = 0.75 - 0.065q_{ij}^{0}$$

$$C = 1+0.055q_{ij}^{0}\exp(-0.023I^{3})$$

$$q_{ij}^0(T) = q_{ij}^0(T_{ref})\left(1 - \frac{T - T_{ref}}{|z_+ z_-|}\right)$$
$$\Gamma_{ij}^0 = (\gamma_i)^{1/z_i^2}$$

where T_{ref} is the reference temperature where $q_{ij}^0(T_{ref})$ is known.

This generalized correlation has many advantages. With only one data point for γ_i at a particular I, one can determine the proper Γ_{ij}^0 curve for that electrolyte for extrapolation (or interpolation) to any other value of I, including those compositions that even exceed the saturation value (solubility) of that particular salt. This feature is particularly valuable for multicomponent systems. Although empirically generated, the Meissner model rigorously follows the Debye-Huckel relationship for $\log_{10} \Gamma_{ij}^0$ at small value of I. A key limitation of the Meissner model is that q_{ij}^0 must be known. One must keep in mind that a minimum of one experimental data point is needed to establish a q_{ij}^0 value.

The Chen Local Composition Model combines Pitzer's extended Debye-Huckel equation for long-range ion-ion interactions with the NRTL model of Renon and Prausnitz for short-range interactions in a local composition framework (59). It is a very nice model. However, it is not practical for the ELM system, as it needs many parameters that are not available.

Since the ionic strength of the aqueous phase of the ELM system is usually less than 0.1M, the Extended Debye-Huckel model and its Davies modified form are suitable and realistic for ELM system. The activity coefficients can be calculated if the concentration of the reactants and products at equilibrium are known. Therefore, in this thesis the Davies modified model is used to calculate the activity coefficients of the aqueous phase of the ELM systems.

Raghuraman and coworkers suggested using the modified Guggenheim equation:

$$\log \gamma_i = -Az_i^2 \frac{I^{0.5}}{1+I^{0.5}} + bI \tag{3.17}$$

Where:

A =0.509;

b = 0.15 for the unmodified equation valid for I<0.1 M. The factor, b, is an adjustable parameter in the modified equation for higher ionic strengths. However for all the predictive models developed here, the standard deviation in the estimated equilibrium constant did not appreciably vary with the b value. Hence a value of 0.15 was used for b throughout (60).

For neutral species, $\log \gamma_i = 0.1I$. (3.18)

And the activity for water is given by: $a_{H_2O} = 1 - 0.017\sum_{i=1}^{n} c_i$ (3.19)

The modified Guggenheim equation is almost the same as the Extended Debye-Huckel model. The only difference is it has one more term, bI, than the Extended Debye-Huckel model. After applying these two models into the ELM systems, we found that the term, bI, in the modified Guggenheim equation was negligible, and the results of the two models were similar. The difference of the modified Guggenheim equation and the Davies modified Debye-Huckel equation is the different parameters of the second term. As the second term is usually much smaller than the first term for the ELM system, the resulting difference is negligible. Thus, all of the three models can be used in the ELM system. In this thesis, the Davis Modified Debye-Huckel equation is used to calculate the activity coefficients in the aqueous phase of the ELM systems.

The activity coefficients of organic phases were investigated. Of the many activity coefficient models for non-electrolytic solutions, the Group contribution model seems the best model for the emulsion liquid membrane system. For a very complicated system as the ELM system, the group contribution model makes the situation even more complicated. It involves many parameters that require complicated thermodynamic experiments. Since this thesis focuses on the behavior of ELM system, the group contribution method was not investigated very deeply. In this thesis, the activity coefficients of the organic phase are assumed to be near one, which means that the organic phase nonidealities are neglected. The reason why organic phase nonidealities may not be significant is due to the fact that the mole fractions of extractant and the metal complex in the organic phase are usually very low (loading< 0.05-0.1) in the ELM system and, hence, activity coefficients of the organic species are close to unity (loading =[organic-metal complex]/[initial extractant]) (60). This approximation may result in minor deviation in the data.

Raghuraman and coworkers also ignored the organic-phase nonidealities in their research initially. If equilibrium constant varies with loading (loading =[organic-metal complex]/[initial D2EHPA dimer]), organic phase nonidealities are lumped and accounted for by fitting an equation for K as a function of loading. For the five metals they studied, only Ni-D2EHPA required this procedure when the loading is bigger than 0.1. For the Cu-LIX systems, a single K value could be used over a large range of pH and ionic strengths. For the Zn-D2EHPA system, a single K value was used for the entire range (60,63).

For the Ni-D2EHPA systems, a single K value was obtained for loading less than one (loading =[organic Ni complex]/[initial D2EHPA dimer]). At higher loadings, the organic phase nonidealities become significant, and the equilibrium constant was fitted as an exponential function of the loading. Organic phase activity coefficients are normally exponential or power functions of component mole fractions, $\log_{10} \gamma = Ax^2$; however, this did not improve or change the predictions (60).

From their research, it can be concluded that for most metals, the equilibrium constant of the interfacial reaction in ELM systems is a constant value. Similar experiments were performed in this study and the results are the same. Assuming the K value as a constant, the following derivation of extraction and stripping coefficients result.

3.3 Extraction and Stripping Distribution Coefficients

3.3.1 Extraction Distribution Coefficient

The reaction at the external-membrane interface:

$$Cu^{2+}(e) + 2RH(m) \Leftrightarrow CuR_2(m) + 2H^+(e) \tag{3.20}$$

$$K = \frac{\gamma_{CuR_{2,m}} [CuR_2]_m \gamma_{H^+,e}{}^2 [H^+]_e^2}{\gamma_{Cu^{2+},e} [Cu^{2+}]_e \gamma_{RH}{}^2 [RH]_m^2} = K_\gamma \frac{[CuR_2]_m [H^+]_e^2}{[Cu^{2+}]_e [RH]_m^2} \tag{3.21}$$

Hence: $[Cu^{2+}]_e = \dfrac{K_\gamma [H^+]_e^2}{K[RH]_m^2} [CuR_2]_m$

Since

$$\left[Cu^{2+}\right]_e = Ce^*$$

$$\left[CuR_2\right]_m = C_m^*$$

$$C_m^* = pC_e^* \qquad (2.3)$$

then:

$$p = K\frac{\left[RH\right]_m^2}{K_\gamma\left[H^+\right]_e^2} \qquad (3.22)$$

As stated earlier, a larger extraction distribution coefficient p means better performance. Equation (3.22) shows that low external hydrogen ion concentration $[H^+]_e$ and high extractant concentration in membrane phase $[RH]_m$ means better performance for copper ion transfer from external phase to membrane phase.

Equation (3.22) is verified by many facts. Wang (1984) experimentally verified that for copper ion extraction, high extractant concentration in membrane phase $[RH]_m$ will perform better (Figure (3.1)) (52).

Zhou (1996) experimentally verified for strontium extraction that pH is reduced gradually in the external phase, or there is hydrogen ion released from membrane phase to the external phase. The experimental curve also shows that when hydrogen ion concentration $[H^+]$ increases in the external phase the value of extraction distribution coefficient p is reduced. Thus the performance of ELM operation shows poor results (Figures (3.2) and (3.3))(29).

In the model calculation, extraction distribution coefficient p is assumed to be a constant and this fact is true when excess extractant RH and buffer are used. When the extractant concentration is much larger than the metal-extractant complex,

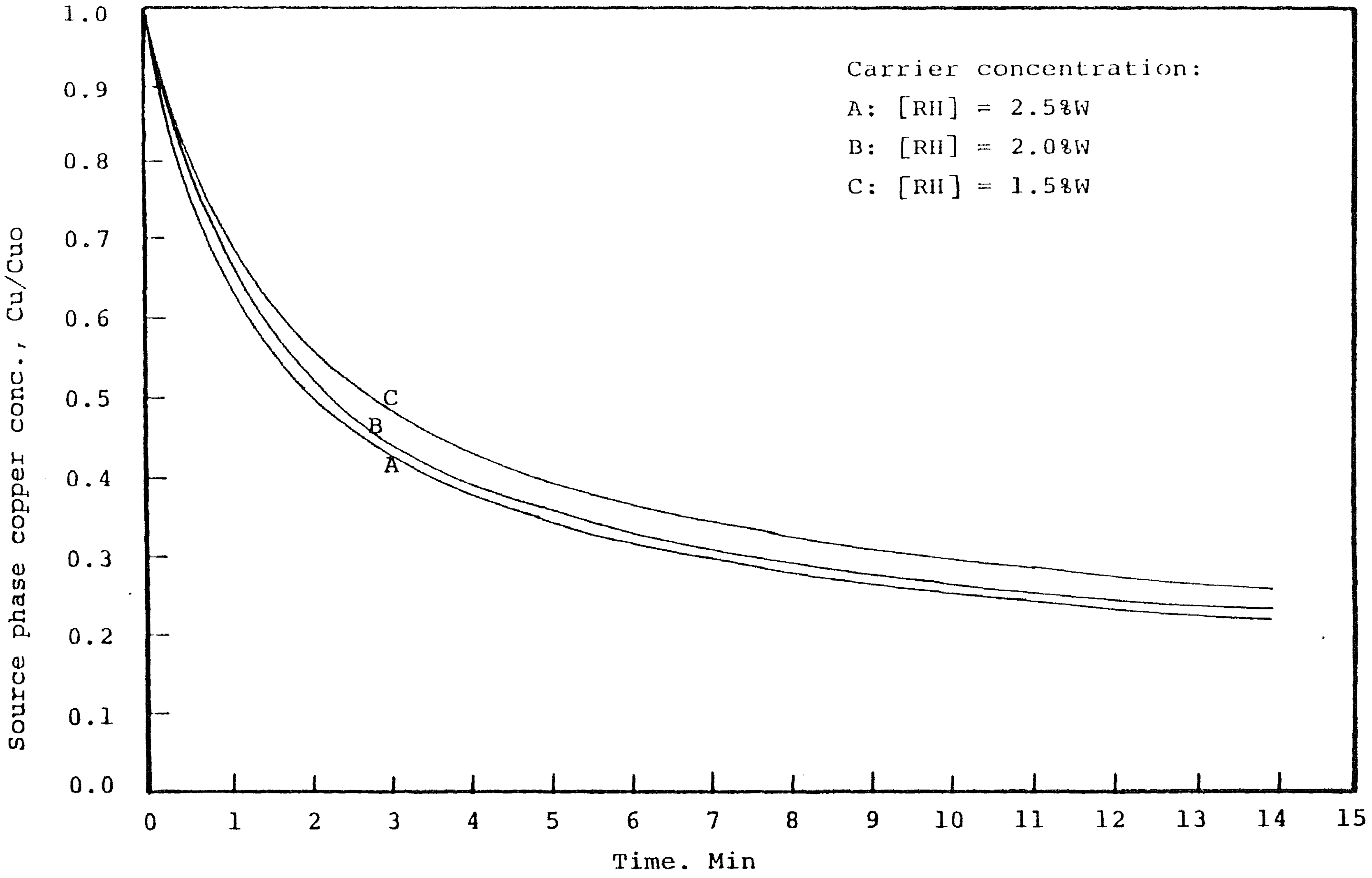

Figure 3.1 Effect of Carrier Concentration on Copper Extraction

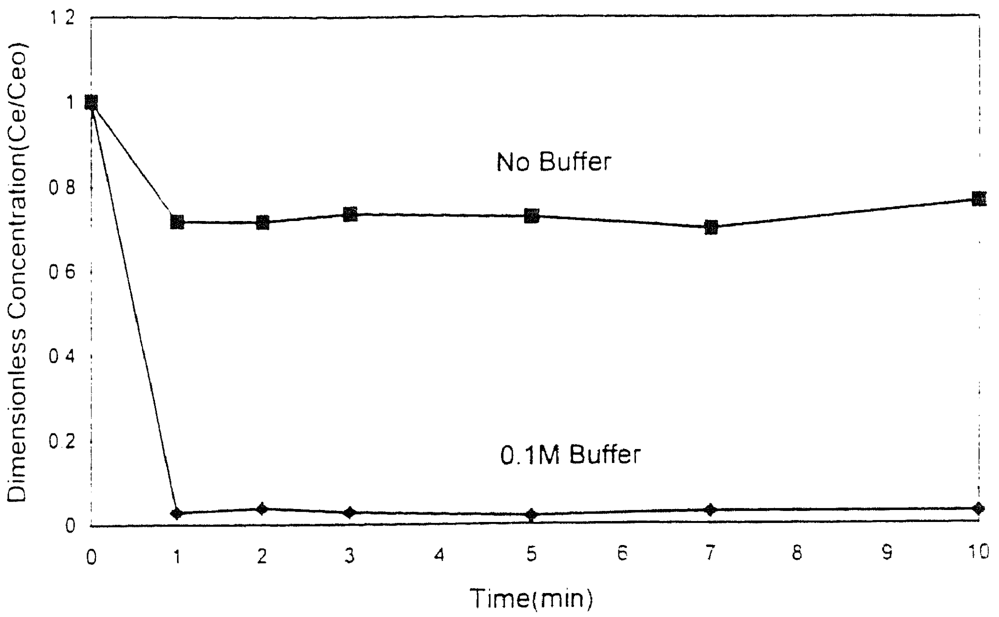

Figure 3.2 Effect of Buffer on Strontium Extraction

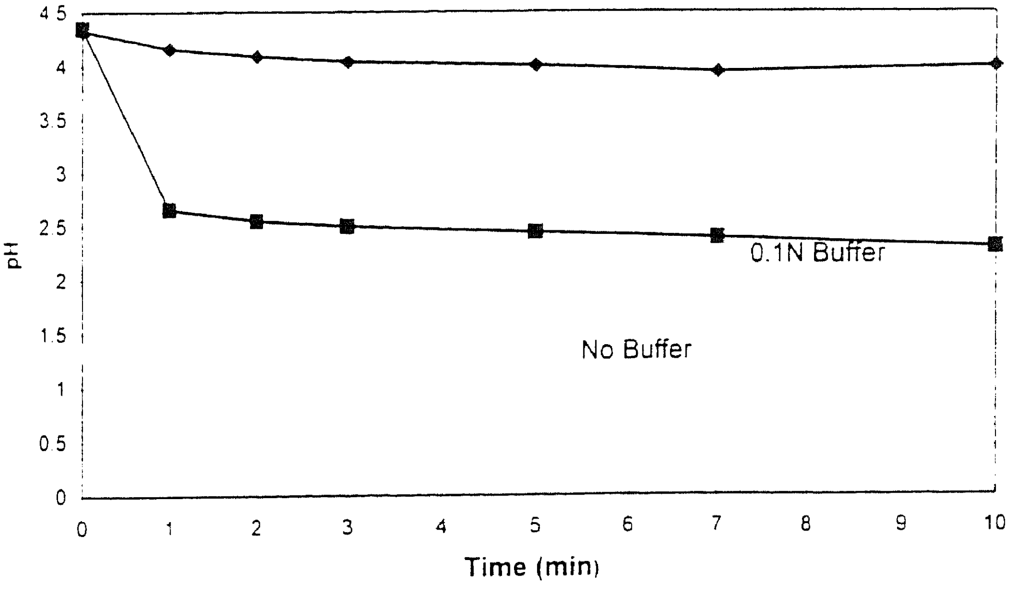

Figure 3.3 The Changes of pH Value During ELM Experiment

[RH]>>[CuR$_2$], the change of extractant concentration [RH] during the reaction is not very large and the concentration of extractant is assumed constant. Hydrogen ion concentration [H$^+$] is almost constant because of the buffer.

3.3.2 Stripping Distribution Coefficient

The reaction at the membrane-internal interface is given by the equation:

$$CuR_2(m) + 2H^+(i) \Leftrightarrow Cu^{2+}(i) + 2RH(m) \tag{3.23}$$

$$K_1 = \frac{\gamma_{Cu,i}^{2+}\left[Cu^{2+}\right]_i \gamma_{RH,m}{}^2\left[RH\right]_m^2}{\gamma_{CuR_2,m}\left[CuR_2\right]_m \gamma_{H_i^+}{}^2\left[H^+\right]_i^2} = K_\gamma{}' \frac{\left[Cu^{2+}\right]_i\left[RH\right]_m^2}{\left[CuR_2\right]_m\left[H^+\right]_i^2} \tag{3.24}$$

The reaction in the internal phase is:

$$Cu^{2+}(i) + SO_4^{2-}(i) \Leftrightarrow CuSO_4(i) \tag{3.25}$$

The equilibrium constant for the above reaction is:

$$K_2 = \frac{\left[CuSO_4\right]_i}{\left[Cu^{2+}\right]_i\left[SO_4^{2-}\right]_i} \tag{3.26}$$

Therefore:

$$\left[Cu^{2+}\right]_i = K_1 \frac{\left[CuR_2\right]_m}{K'_\gamma\left[RH\right]_m^2}\left[H^+\right]_i^2$$

$$\left[CuSO_4\right]_i = K_2\left[Cu^{2+}\right]_i\left[SO_4^{2-}\right]_i$$

Since

$$C_i^* = C_i = qC_{mi}^* = qC_m \tag{2.5}$$

Since C_i^* includes all forms of Cu in the internal phase,

$$C_i = [Cu^{2+}]_i + [CuSO_4]_i \tag{3.27}$$

$$C_i = K_1 \frac{[CuR_2]_m}{K'_\gamma [RH]_m^2}[H^+]_i^2 + K_2 K_1 \frac{[CuR_2]_m}{K'_\gamma [RH]_m^2}[H^+]_i^2 [SO_4^{2-}]_i$$

$$C_i = \frac{[CuR_2]_m}{K'_\gamma [RH]_m^2}[H^+]_i^2 \{K_1 + K_1 K_2 [SO_4^{2-}]_i\}$$

$$C_m = [CuR_2]_m$$

Therefore:

$$q = \frac{[H^+]_i^2}{K_\gamma' [RH]_m^2} \{K_1 + K_1 K_2 [SO_4^{2-}]_i\} \tag{3.28}$$

Equation (3.28) shows that high internal $[H^+]$ and low extractant [RH] will enhance the performance of $[Cu^{++}]$ transfer from the membrane phase to the internal phase. Wang (1984) shows that increasing the internal phase nitric acid concentration gives a higher value of q, and therefore better ELM performance (Figure (3.4))(52).

Equation (3.28) shows that for better performance, $[RH]_m$ should be small and equation (3.22) shows that for better performance, $[RH]_m$ should be large. This means that an accurate important optimum value of $[RH]_m$ should be determined in Cu^{++} extraction by ELM.

3.4 Impact of Internal Phase Chemical Reactions on the Mass Transport Model

In the previous model, chemical reaction in the internal phase was not considered (29, 52). When the metal ion is transferred into the internal phase, it does not simply stay in the internal aqueous phase as assumed before. The metal ion will react with the salt ion

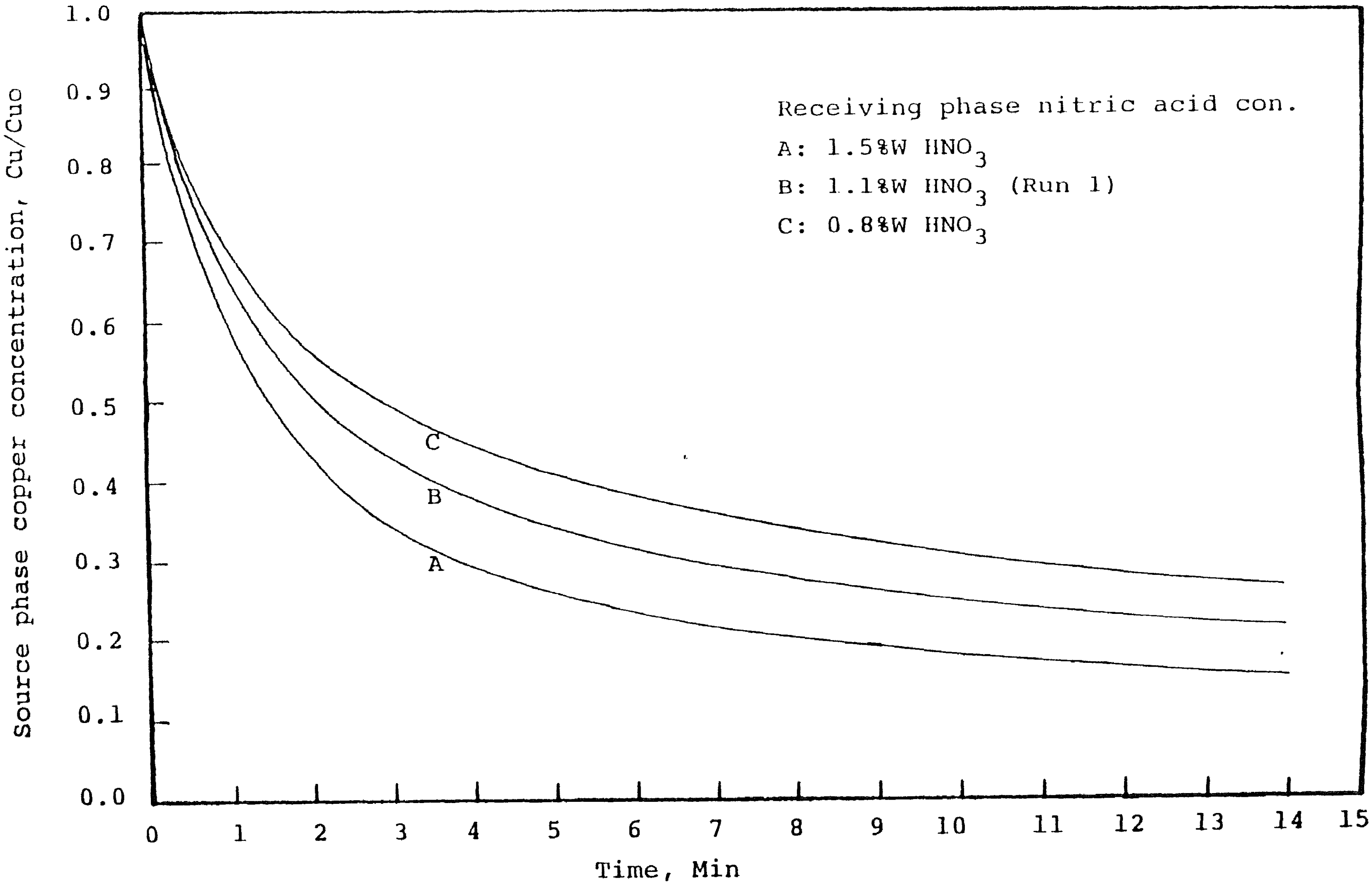

Figure 3.4 Effect of Receiving Phase Concentration on Copper Extraction

in the internal phase to form salt. Some of the salt is not soluble and, hence, the concentration of metal ion in the internal phase is smaller than when the chemical reaction is not considered. In this situation, the mass transfer rate should be larger because the driving force, the concentration difference of the metal in the two phases, is bigger. Considering the internal phase chemical reactions, mass transfer can be described by a mathematical model.

The example used is the extraction of copper with extractant LIX-64N (octanol) in the membrane phase and sulfuric acid solution in the internal phase. The following equations result:

1. ***External phase mass transfer resistance from external phase to the external-membrane interface***

$$V_e \frac{dC_e}{dt} = -N(4\pi R^2)k(C_e - C_e^*) \tag{2.1}$$

when t =0, $C_e = C_{e0}$ for all r

2. ***Mass fluxes at the external-membrane interface***

$$N(4\pi R^2)k(C_e - C_e^*) = N(4\pi R^2)D_e\left(\frac{\partial C_m}{\partial r}\right)_{r=R} \tag{2.2}$$

3. ***Equilibrium at the external-membrane interface***

$$C_{me}^* = pC_e^* \tag{2.3}$$

where C_{me}^* = the concentration of the metal-extractant complex in the membrane phase at the interface (or at r=R) of membrane and external phase

4. ***Mass transfer inside a droplet of membrane phase with water-in-oil emulsion of internal phase***

$$V_m \frac{\partial C_m}{\partial t} = (V_m + V_i)D_e \frac{1}{r^2}\frac{\partial}{\partial r}\left(r^2 \frac{\partial C_m}{\partial r}\right) - V_i \frac{\partial C_{it}}{\partial t} \tag{2.4}$$

Initial condition: $C_m = 0$ for all r, when t = 0

Boundary conditions: C_m = finite, when r = 0; $C_m = C_{me}^*$, when r = R

$$C_{it} = C_i + C_{is} \tag{3.29}$$

where C_{it} = total concentration of metal in the internal phase

C_i = concentration of metal ion in the internal phase (mol/l)

C_{is} = concentration of metal salt in the internal phase (mol/l)

5. ***Equilibrium at internal-membrane interface***

$$C_i^* = C_i = qC_{mi}^* = qC_m \tag{2.5}$$

Initial condition: $C_i = 0$, when t = 0

Where C_{mi}^* = concentration of metal-extractant complex at the membrane-internal interface

All other variables are the same with those in Chapter 2, Section 2.2.

Since the chemical reactions in the ELM systems are being modeled, an example of a specific system must be considered. The example is extraction of copper with extractant LIX-64N(octanol) in the membrane phase and sulfuric acid solution in the internal phase.

The reaction at external-membrane interface is:

$$Cu^{2+}(e) + 2RH(m) \Leftrightarrow CuR_2(m) + 2H^+(e) \tag{3.20}$$

The equilibrium constant of above reaction is the following:

$$K = \frac{\gamma_{CuR_{2},m} [CuR_2]_m \gamma_{H^+,e}{}^2 [H^+]_e^2}{\gamma_{Cu^{2+},e} [Cu^{2+}]_e \gamma_{RH}{}^2 [RH]_m^2} = K_\gamma \frac{[CuR_2]_m [H^+]_e^2}{[Cu^{2+}]_e [RH]_m^2} \tag{3.21}$$

The reaction at membrane-internal interface is:

$$CuR_2(m) + 2H^+(i) \Leftrightarrow Cu^{2+}(i) + 2RH(m) \tag{3.23}$$

The equilibrium constant of above reaction is the following:

$$K_1 = \frac{\gamma_{Cu^{2+}_{,i}}[Cu^{2+}]_i \gamma_{RH,m}^{2}[RH]_m^2}{\gamma_{CuR_2,m}[CuR_2]_m \gamma_{H^+_{,i}}^{2}[H^+]_i^2} = K_\gamma \frac{[Cu^{2+}]_i [RH]_m^2}{[CuR_2]_m [H^+]_i^2} \tag{3.24}$$

The chemical reaction in the internal phase is:

$$Cu^{2+}(i) + SO_4^{2-}(i) \Leftrightarrow CuSO_4(i) \tag{3.25}$$

The equilibrium constant of above equation is:

$$K_2 = \frac{[CuSO_4]_i}{[Cu^{2+}]_i [SO_4^{2-}]_i} \tag{3.26}$$

The total concentration of metal ions in the internal phase $C_{it} = C_i + C_{is}$.

In this example: $C_{it} = Cu^{2+}(i) + CuSO_4(i)$ (3.27)

$$C_i = Cu^{2+}(i)$$

$$C_{is} = CuSO_4(i) = K_2[SO_4^{2-}]_i [Cu^{2+}]_i = K_2[SO_4^{2-}]_i C_i$$

and, hence,

$$C_{it} = (1 + K_2[SO_4^{2-}]_i)C_i = (1 + K_2[SO_4^{2-}]_i)qC_m \tag{3.30}$$

Equation (2.4) becomes:

$$V_m \frac{\partial C_m}{\partial t} = (V_m + V_i)D_e \frac{1}{r^2}\frac{\partial}{\partial r}(r^2 \frac{\partial C_m}{\partial r}) - V_i \frac{\partial(1 + K_2[SO_4^{2-}]_i)qC_m}{\partial t} \tag{3.31}$$

Rearranging the above equation gives:

$$\frac{V_m + (1 + K_2[SO_4^{2-}]_i)qV_i}{(V_m + V_i)} \frac{\partial C_m}{\partial t} = D_e \frac{1}{r^2}\frac{\partial}{\partial r}(r^2 \frac{\partial C_m}{\partial r}) \tag{3.32}$$

Changing the above equations into dimensionless form gives:

External: $\frac{dU_e}{\partial\tau} = -K_0(U_e - U_e^*)$ (2.15)

$G(\frac{\partial U_m}{\partial \nu})|_{\nu=1} = (U_e - U_e^*)$ (2.16)

Equilibrium: $U_e^* = U_m^*$ (2.17)

Initial condition: $U_e = U_e^* = 1$ when $\tau = 0$ (2.18)

Membrane: $\omega\frac{\partial U_m}{\partial\tau} = \frac{1}{\nu^2}\frac{\partial}{\partial\nu}(\nu^2\frac{\partial C_m}{\partial\nu})$ (2.19)

Initial conditions: $U_m = 0$, when $\tau = 0$ (2.20)

Boundary conditions: $U_m = \mathit{finite}$ when $\nu = 0$ (2.21)

$U_m = U_e^*$ when $\nu = 1$ (2.22)

where

$$\omega = 1 - e + e((1 + K_2[SO_4^{2-}]_i)q) = \frac{V_m + (1 + K_2[SO_4^{2-}]_i)qV_i}{(V_m + V_i)} \quad (3.33)$$

$$p = K\frac{[RH]_m^2}{[H^+]_m^2} \quad (3.22)$$

$$q = \frac{[H^+]_i^2}{[RH]_m^2}\{K_1 + K_1K_2[SO_4^{2-}]_i\} \quad (3.28)$$

Other variables are the same with those in Chapter 2, Section 2.2. The procedure to solve the above equations is the same with that in Chapter 2, Section 2.2. The detailed mathematical steps are omitted and final analytical solutions are given.

The metal ion concentration profile in the external phase is:

$$U_e = \frac{C_e}{C_{e0}} = \frac{3}{B+3} + \sum_{n=1}^{\infty} \frac{2B}{3B + B^2 + b_n^2 + Gb_n^2(Gb_n^2 - 2B - 1)} \exp(-\frac{b_n^2}{\omega}\tau) \qquad (2.24)$$

The metal ion concentration profile at the external-membrane interface is:

$$U_e^* = \frac{C_e^*}{C_{e0}} = \frac{3}{B+3} + \sum_{n=1}^{\infty} \frac{2(B - Gb_n^2)}{3B + B^2 + b_n^2 + Gb_n^2(Gb_n^2 - 2B - 1)} \exp(-\frac{b_n^2}{\omega}\tau) \qquad (2.25)$$

The metal-extractant concentration profile in the membrane phase is:

$$U_m = \frac{C_m}{pC_{e0}} = \frac{3}{B+3} + \sum_{n=1}^{\infty} \frac{2(B - Gb_n^2)(\frac{\sin(b_n * v)}{v * \sin(b_n)})}{3B + B^2 + b_n^2 + Gb_n^2(Gb_n^2 - 2B - 1)} \exp(-\frac{b_n^2}{\omega}\tau) \qquad (2.23)$$

With the concentration profile of membrane phase, the concentration profile in internal phase can be found with equation (2.5), $C_i^* = C_i = qC_{mi}^* = qC_m$.

The metal ion concentration profile in internal phase is:

$$\frac{C_i}{pqC_{e0}} = \frac{3}{B+3} + \sum_{n=1}^{\infty} \frac{2(B - Gb_n^2)(\frac{\sin(b_n * v)}{v * \sin(b_n)})}{3B + B^2 + b_n^2 + Gb_n^2(Gb_n^2 - 2B - 1)} \exp(-\frac{b_n^2}{\omega}\tau) \qquad (3.34)$$

Since $C_{is} = CuSO_4(i) = K_2[SO_4^{2-}]_i[Cu^{2+}]_i = K_2[SO_4^{2-}]_i C_i$

The metal salt concentration profile in internal phase is:

$$\frac{C_{is}}{K_2\left[SO_4^{2-}\right]_i pqC_{e0}}=\frac{3}{B+3}+\sum_{n=1}^{\infty}\frac{2(B-Gb_n^2)(\frac{\sin(b_n*v)}{v*\sin(b_n)})}{3B+B^2+b_n^2+Gb_n^2(Gb_n^2-2B-1)}\exp(-\frac{b_n^2}{\omega}\tau) \quad (3.35)$$

The total metal concentration profile in internal phase can be obtained by combining equations (3.34) and (3.35).

The variables are the same with those in Chapter 2, Section 2.2, except the dimensionless group ω, the extraction distribution coefficient, p, and the stripping distribution coefficient, q. Equation (3.33) is the new expression for dimensionless group ω. The extraction distribution coefficient, p, and stripping distribution coefficient, q, are no longer input parameters determined by experiments. Equation (3.22) and equation (3.28) give their theoretical expressions.

Extraction of cadmium is used as an example to illustrate the impact of internal phase reaction. The external phase is 500ml with 1000ppm Cd^{2+}. The initial pH value is 3.8. The membrane phase is 41ml of 5% D2EHPA as extractant and Exxol D-80 as diluent. The internal phase is 9ml of 3M H_2SO_4.

The external concentration profile for this system considering internal phase reaction is shown in Figure 3.5 as a solid line. The external concentration profile without considering internal phase reaction is the dot line. The curve shows that the two lines do not have much difference within finite time. The dimensionless group ω is much bigger when we consider the internal phase reaction. This results the dimensionless time, τ=t/ω, being smaller. Thus, the corresponding dimensionless time to this experiment period,

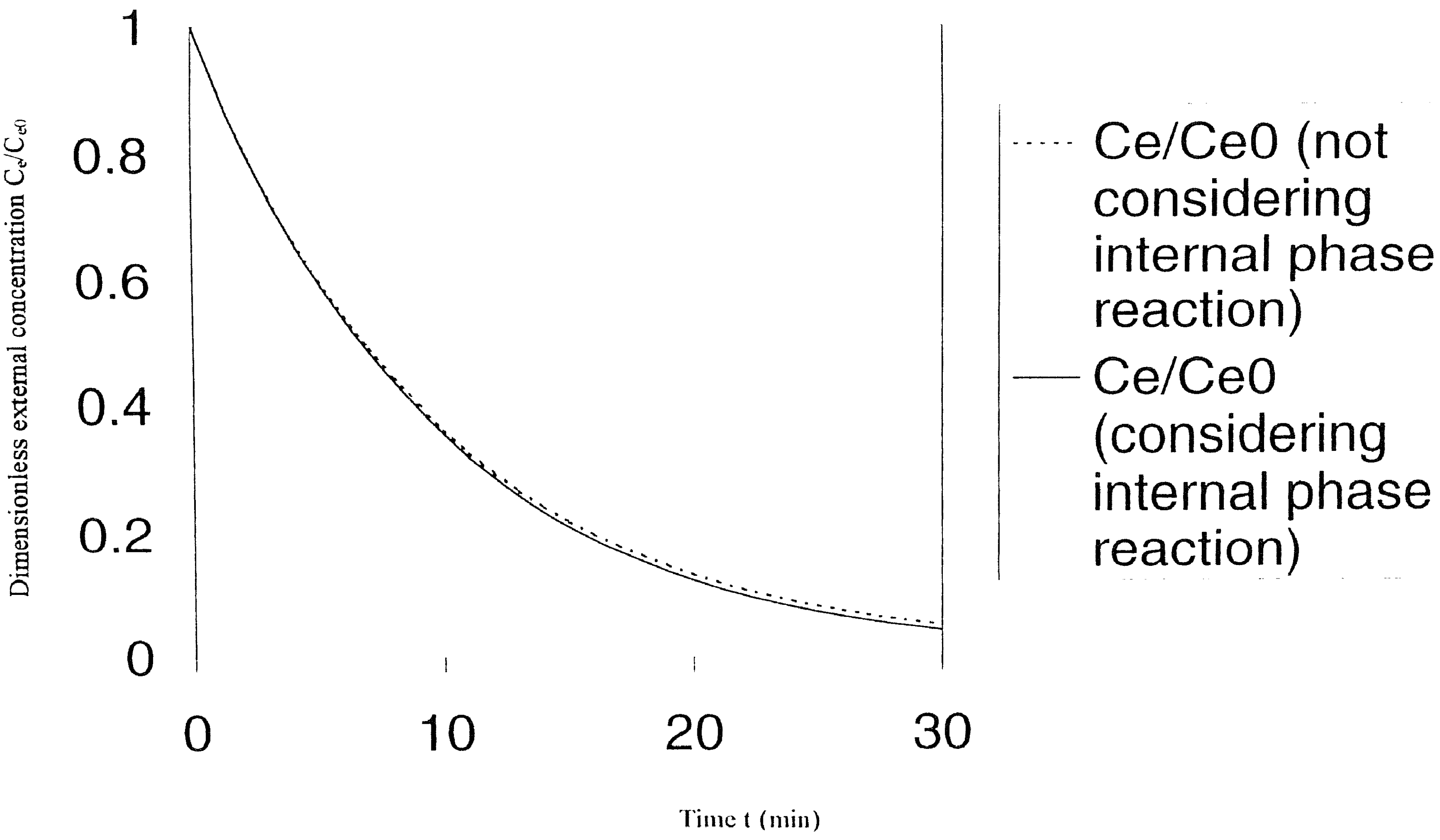

Figure 3.5 External Concentration Profiles Considering and Not Considering Internal Phase Chemical Reaction

30 minutes, is relatively small. As a consequence, the difference between the two concentration profiles is not significant.

However, when time approaches to infinity, the solute concentrations at equilibrium are different. The dimensionless concentration when time goes to infinity is:

$$\frac{C_{e\infty}}{C_{e0}} = \frac{3}{B+3} \tag{2.32}$$

The internal phase reaction is not considered and the value of emulsion capacity B=1700 is calculated. In this case, the external dimensionless concentration at equilibrium is $\frac{C_{e\infty}}{C_{e0}} = 0.00176$.

Considering the internal phase reaction, one can get emulsion capacity is B=5.0*10^8 and the external dimensionless concentration at equilibrium is $\frac{C_{e\infty}}{C_{e0}} = 2 \times 10^{-9}$.

The difference of the external phase equilibrium concentration shows the impact of the internal reaction. The model shows that the internal reaction increases the driving force of the mass transport in ELM systems and enhances the performance of the ELM system. This is true because the internal reaction decreases the metal ion concentration in the internal phase, thus, increasing the driving force for the metal transport from the external phase to the internal phase. Therefore the performance of the ELM is better. However, the impact of the internal phase is not significant when applied to engineering practices.

CHAPTER 4

EXPERIMENTAL VERIFICATION OF MATHEMATICAL MODEL

4.1 Verification Methodology

Copper extraction is used as an illustration to show the methodology. Copper is extracted with extractant LIX-64N (octanol) in the membrane phase and sulfuric acid solution in the internal phase.

4.1.1 Evaluation of the Extraction Distribution Coefficient p and the Stripping Distribution Coefficient q Theoretically

The reaction at the external-membrane interface is:

$$Cu^{2+}(e) + 2RH(m) \Leftrightarrow CuR_2(m) + 2H^+(e) \tag{3.20}$$

As previously discussed, the equilibrium constant is:

$$K = \frac{\gamma_{CuR_2,m}[CuR_2]_m \gamma_{H^+_{,e}}^2 [H^+]_e^2}{\gamma_{Cu^{2+}_{,e}}[Cu^{2+}]_e \gamma_{RH,m}^2 [RH]_m^2} = K_\gamma \frac{[CuR_2]_m [H^+]_e^2}{[Cu^{2+}]_e [RH]_m^2} \tag{3.21}$$

and extraction distribution coefficient is:

$$p = K \frac{[RH]_m^2}{K_\gamma [H^+]_m^2} \tag{3.22}$$

The lumped activity coefficients are theoretically predicted with the Davies modified Debye-Huckel model. The extraction distribution coefficient p is calculated with equation (3.22).

The reaction at the membrane-internal interface is:

$$CuR_2(m) + 2H^+(i) \Leftrightarrow Cu^{2+}(i) + 2RH(m) \tag{3.23}$$

The equilibrium constant is:

$$K_1 = \frac{\gamma_{Cu^{2+}_{,i}} \left[Cu^{2+}\right]_i \gamma_{RH,m}^{\,2} \left[RH\right]_m^2}{\gamma_{CuR_2,m} \left[CuR_2\right]_m \gamma_{H^+_{,i}}^{\,2} \left[H^+\right]_i^2} = K_\gamma \frac{\left[Cu^{2+}\right]_i \left[RH\right]_m^2}{\left[CuR_2\right]_m \left[H^+\right]_i^2} \tag{3.24}$$

The reaction in the internal phase is:

$$Cu^{2+}(i) + SO_4^{2-}(i) \Leftrightarrow CuSO_4(i) \tag{3.25}$$

The equilibrium constant for the above equation is:

$$K_2 = \frac{\left[CuSO_4\right]_i}{\left[Cu^{2+}\right]_i \left[SO_4^{2-}\right]_i} \tag{3.26}$$

As shown in Chapter 3,equation (3.28), the stripping distribution coefficient is:

$$q = \frac{\left[H^+\right]_i^2}{K_\gamma \left[RH\right]_m^2} \{K_1 + K_1 K_2 \left[SO_4^{2-}\right]_i\} \tag{3.28}$$

4.1.2 Evaluation of Extraction Distribution Coefficient p and Stripping Distribution Coefficient q with Single-stage Equilibrium Experiments

By definition, the extraction distribution coefficient $p = \dfrac{\left[CuR_2\right]_m}{\left[Cu^{2+}\right]_e}$ (4.1)

A one-stage equilibrium operation with mixing and then settling in a closed vessel with equal volumes of external phase and organic phase (membrane phase without internal phase in it) is used to get the equilibrium concentration of the metal ion in the external phase. A mass balance is used to get the equilibrium concentration of metal-extractant complex. Using equation (4.1), the extraction distribution coefficient can be calculated.

By definition, the stripping distribution coefficient is $q = \dfrac{\left[Cu^{2+}\right]_e}{\left[CuR_2\right]_m}$ (4.2)

A one-stage equilibrium operation with mixing and then settling in a closed vessel with equal volumes of internal phase and organic phase is used to find the stripping distribution coefficient q.

4.1.3 Calculate the Extraction and the Stripping Distribution Coefficients p and q from ELM Experiments

The extraction and stripping coefficients p and q are calculated from the experimental data of ELM system. An ELM experiment is made to measure the concentrations as functions of time. The set of extraction and stripping distribution coefficients p and q values are determined producing the theoretical concentration profile that best matches the experimental data. The resulting values of p and q are compared with the values obtained from the theoretical prediction.

4.2 Measurement of Stoichiometric Coefficients and Equilibrium Constant

For any metal ion that is to be removed from water with the ELM systems, it is necessary to first know the chemical reactions at the interface and the stoichiometric coefficients of the reaction. Only after these are known, can the equilibrium constant, extraction and stripping distribution coefficients be predicted. Therefore, initially the interfacial reactions and stoichiometry were studied.

The theory of the equilibrium constant was studied in Chapter 3, section 3.2. In this chapter, it can be verified experimentally that the equilibrium constant can be written in the traditional way. Therefore, two kinds of experiments on these two issues are performed prior to proceeding the extraction and the stripping distribution coefficients.

4.2.1 Stoichiometric Studies

4.2.1.1 Experimental Design: It is desired to recover the metal ion M^{2+} in the wastewater with the emulsion liquid membrane system. The extractant (carrier) in the membrane phase is the Di(2-Ethylhexyl)-Phosphoric Acid (D2EHPA), or simplify RH. The reaction at the external-membrane interface is:

$$M^{2+}(e) + \tfrac{1}{2}n(RH)_2(m) \Leftrightarrow MR_2(n-2)RH(m) + 2H^+(e) \tag{4.3}$$

It is desired to know what the value of n should be in such a reaction. Once the value of n is determined, the equilibrium constant and extraction distribution coefficient and stripping distribution coefficient can be evaluated. There is an empirical method to determine the value of n (64). Using Cd^{2+} as an example,

$$Cd^{2+}(e) + \tfrac{1}{2}n(RH)_2(m) \Leftrightarrow CdR_2(n-2)RH(m) + 2H^+(e) \tag{4.4}$$

If the ionic strength in the aqueous medium is kept constant, the activity coefficients of the species do not change during the reaction. The equilibrium constant is in the following form:

$$K = \frac{[CdR_2(n-2)HA]_m [H^+]_e^2}{[Cd^{2+}]_e [(RH)_2]_m^{\frac{n}{2}}} \tag{4.5}$$

The extraction distribution coefficient p is:

$$p = \frac{[CdR_2(n-2)HA]_m}{[Cd^{2+}]_e} \tag{4.6}$$

Therefore, the relationship between the equilibrium constant and extraction distribution coefficient is obtained:

$$K = \frac{p[H^+]_e^2}{[(RH)_2]_m^{\frac{n}{2}}} \tag{4.7}$$

Taking the logarithm of equation (4.7) yields:

$$LogK = Logp + 2\log[H^+]_e - \tfrac{n}{2}\log[(RH)_2]_m$$

or:

$$Logp = LogK + 2pH + \tfrac{n}{2}\log[(RH)_2]_m \tag{4.8}$$

If the volumes of the organic phase and the aqueous phase are equal, then:

$$[CdR_2(n-2)HA]_m = [Cd^{2+}]_0 - [Cd^{2+}]_e \tag{4.9}$$

From the stoichiometry of the reaction:

$$[(RH)_2]_m = \tfrac{1}{2}[RH]_0 - \tfrac{1}{2}n[CdR_2(n-2)HA]_m \tag{4.10}$$

If the initial extractant concentration $[RH]_0$ is much greater than the concentration of the metal-extractant complex $[CdR_2(n\text{-}2)HA]_m$, the above equation shows that the equilibrium extractant concentration $[(RH)_2]_m$ can be approximated as a constant of ½ $[RH]_0$.

Equation (4.8) shows that , at constant pH, a plot of log[p] against log $[(RH)_2]$ gives a straight line of slope equal to ½ n.

The experiments are designed to determine the dependence of the extraction distribution coefficient on the D2EHPA concentration. From the straight line, the stoichiometric coefficient n can be obtained.

4.2.1.2 Experiments: Each sample consists of 10ml volume of each phase in a one-inch closed specimen tube. The membrane phase consists of extractant Di(2-Ethylhexyl)-Phosphoric Acid (D2EHPA) and Exxol D-80. Exxol D-80 consists predominantly of C12-C14 saturated hydrocarbons. The concentrations of D2EHPA of different samples are different. The aqueous phase is a buffer solution with Cd^{2+}. The buffer is a solution of Na_2HPO_4 and Citric Acid. The samples are shaken using a magnetic stirrer for 24 hours. Then the sample is allowed to settle and separate. The temperature is room temperature. The concentration of cadmium ion in the aqueous phase is measured using an atomic absorption spectrophotometer at the wavelength of 228.8nm. The organic phase concentrations are found by difference (29).

4.2.1.3 Results: The extraction of cadmium ion from the aqueous phase to the membrane phase with extractant concentration of D2EHPA of 0.005 kmol/m3, 0.025, and 0.05 respectively is investigated. The results are potted in Figure 4.1. The straight line is obtained by the least squares method. The correlation coefficient R= 0.9995. The slope of this line is 2.50225 which means ½ n=2.5, and, therefore, n=5. This result suggests that the stoichiometry of the overall reaction is:

$$Cd^{2+}(e) + 2.5(RH)_2(m) \Leftrightarrow CdR_2 \cdot 3RH(m) + 2H^+(e) \tag{4.11}$$

This is the same result of previous work on the cadmium ion (63).

4.2.2 Equilibrium Constant Studies

4.2.2.1 Experimental Design: Using cadmium as an example,

$$Cd^{2+}(e) + 2.5(RH)_2(m) \Leftrightarrow CdR_2 \cdot 3RH(m) + 2H^+(e) \tag{4.11}$$

$$K = \frac{\gamma_{CdR_2 \cdot 3RH,m} \left[CdR_2 \cdot 3RH\right]_m \gamma_{H^+,e}{}^2 \left[H^+\right]_e^2}{\gamma_{Cu^{2+},e} \left[Cd^{2+}\right]_e \gamma_{RH}{}^{2.5} \left[(RH)_2\right]_m^{2.5}} = K_\gamma \frac{\left[CdR_2 \cdot 3RH\right]_m \left[H^+\right]_e^2}{\left[Cd^{2+}\right]_e \left[(RH)_2\right]_m^{2.5}} \tag{4.12}$$

The activity coefficients of organic phase are considered to be one.

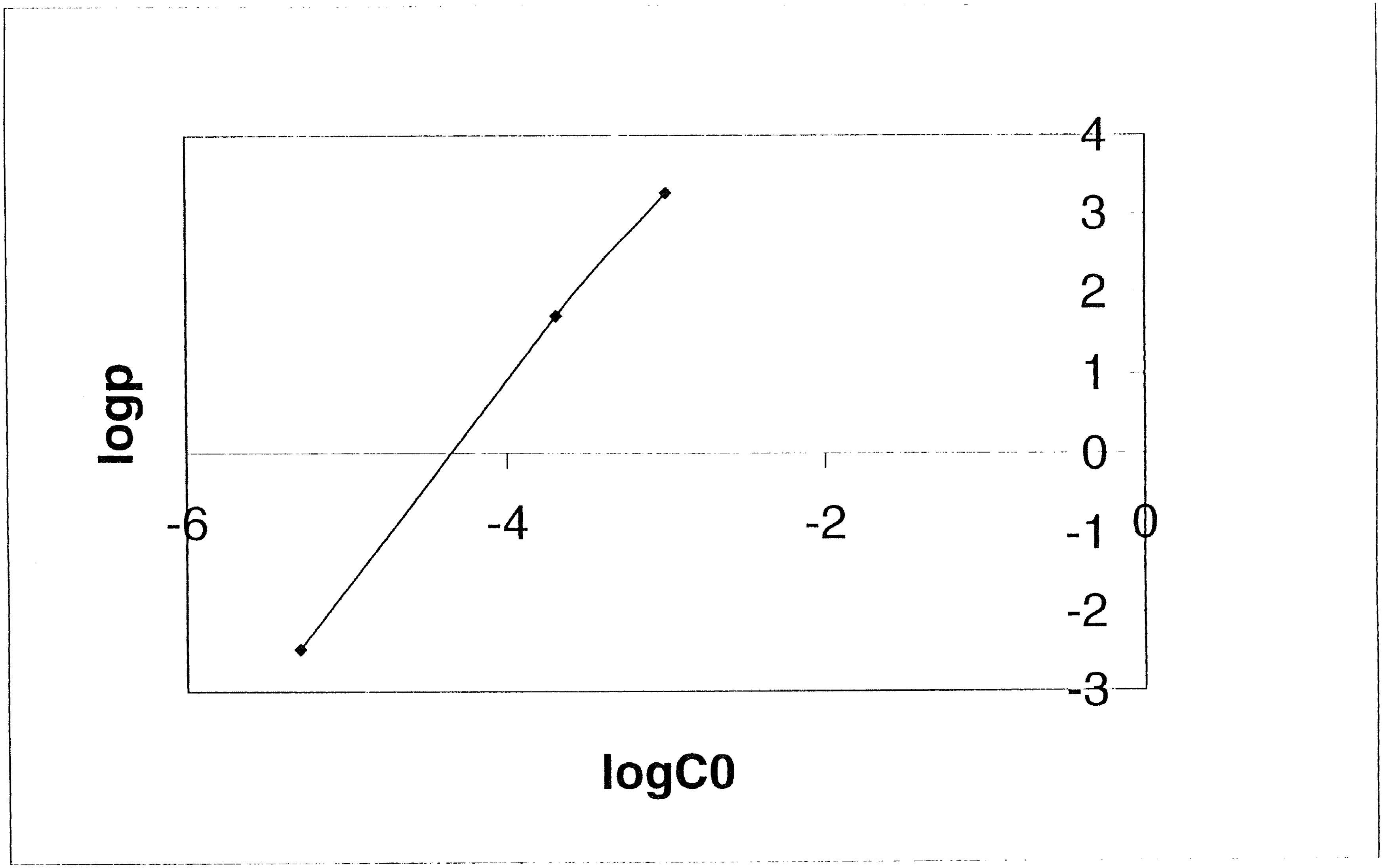

Figure 4.1 Extraction Distribution Coefficient as a Function of Initial Extractant Concentration

The aqueous phase activity coefficients are calculated by Davies modified Debye-Huckel model: $\log_{10}\gamma_i = -Az_i^2(\frac{I^{1/2}}{1+I^{1/2}} - 0.3I)$ (3.13)

Where I = the ionic strength of solution

$$I = \tfrac{1}{2}\sum_{i=1}^{n} c_i z_i^2 \qquad (3.16)$$

z_i = the ionic charge;

c_i = the concentration of ionic species;

A = 0.509;

The equilibrium concentrations are measured and entered into equation (4.12) to verify that K is a constant.

4.2.2.2 Experiments: The source for cadmium ion is Cadmium sulfate from Sigma. The extractant is D2EHPA from Sigma. Solvent is Exxol D-80 from Novick Chemical Company. Water is deionized (DI) water. Aqueous solutions of metal ions are prepared by dissolving the cadmium sulfate into deionized water. The initial metal ion concentration is set at about 1000ppm. The pH value is adjusted by sodium acetate-acetic acid buffer. The organic phase contains 5% by volume extractant (carrier) D2EHPA and 95% by volume Exxol D-80 as a diluent.

Equilibrium distribution experiments require contacting known volumes of aqueous phase and organic phase in an Erlenmeyer flask with agitation for about 2 hours at room temperature(60). Ten ml of aqueous phase and 10ml of organic phase mentioned above are placed into a closed Erlenmeyer flask with a magnetic stirrer for 24 hours. The two phases are separated with separatory funnel and the pH of the aqueous phase is measured with a pH meter. The metal ion concentration in the aqueous phase is measured with flame atomic absorption spectroscopy with the wavelength of 228.8nm. The organic phase metal ion concentration is calculated by material balance.

4.2.2.3 Results and Discussion: Figure 4.2 shows extraction of cadmium ion with 5% D2EHPA as a function of pH. The aqueous phase is 10 ml of 1000ppm Cd^{2+}, with the pH to be adjusted by NaAc-HAc buffer. The organic phase contains 5% volume D2EHPA and 95% volume Exxol D-80.

Equation (4.11), (4.12) together with mass balance equations and Davies modified Debye-Huckel model are solved for experimental data. Each data set gives a value of the equilibrium constant, K. The average K value is calculated to be 0.0258. This agrees with the results of Raghuraman and coworker's(63). However, some data points at the extremes of the extraction curves are excluded since even small errors in aqueous phase concentration measurement could lead to large errors in the estimating of the equilibrium constant, K.

4.3 Single-stage Measurements of Extraction and Stripping Distribution Coefficients

4.3.1 Single–stage Measurements of Extraction Distribution Coefficients, p

Aqueous solutions of metal ions are prepared by dissolving cadmium sulfate in deionized water. The initial metal ion concentration is set at about 1000ppm. The pH value is adjusted by a sodium acetate-acetic acid buffer. The organic phase contains 5% volume extractant (carrier) D2EHPA and 95% volume Exxon D-80.

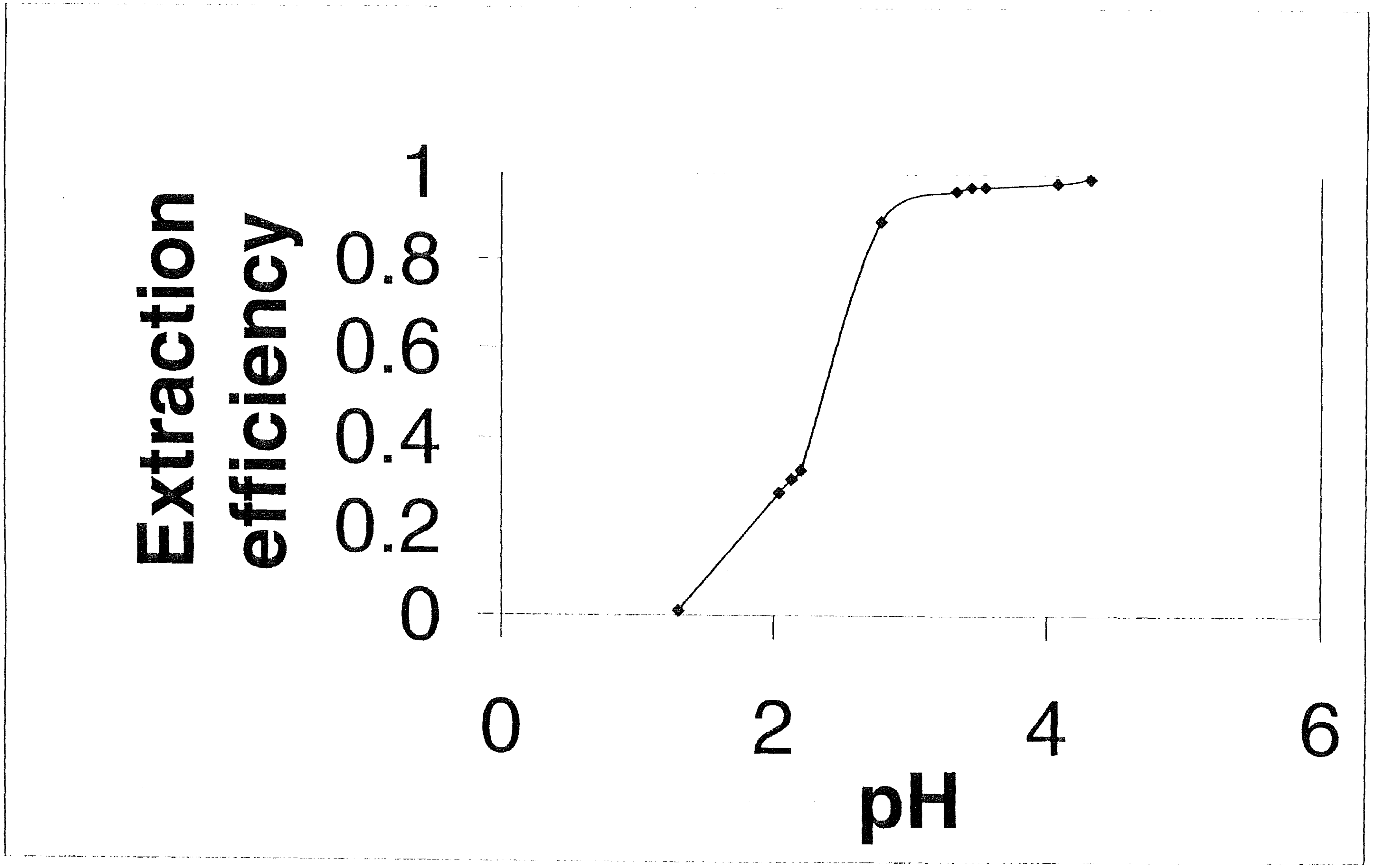

Figure 4.2 Efficiency of Cadmium Equilibrium Extraction as a Function of pH Value

Ten ml aqueous phase and 10ml organic phase are placed into a closed test tube with magnetic stirring. After 24 hours, the two phases are separated. The pH of the aqueous phase is measured. The metal concentration in the aqueous phase is measured with flame atomic absorption spectroscopy with the wavelength of 228.8nm. The organic phase metal ion concentration is calculated by material balance.

Based on the definition, the extraction distribution coefficient can be calculated

$$p = \frac{[CdR_2 \cdot 3RH]_m}{[Cd^{2+}]_e}.$$

4.3.2 Single–stage Measurements of Stripping Distribution Coefficients, q

The aqueous phase is 3M H_2SO_4 and the initial cadmium ion concentration is 1000ppm. The organic phase is 5% volume D2EHPA and 95% Exxol D-80. Ten ml aqueous phase and 10ml organic phase are mixed with magnetic stirring for 24 hours to ensure that the reaction reaches equilibrium. Then the sample is allowed to settle and the two phases are separated with a separatory funnel. The pH of the aqueous phase is measured. The metal ion concentration in the aqueous phase is measured with flame atomic absorption spectroscopy with the wavelength of 228.8nm. The organic phase metal ion concentration is calculated by material balance.

By definition, the stripping distribution coefficient, $q = \frac{[CdR_2 \cdot 3RH]_m}{[Cd^{2+}]_i}$, and, hence, the stripping distribution coefficient, q, can be calculated, knowing the equilibrium concentrations of metal ion in the membrane phase and in the internal phase.

4.4 Evaluate Extraction and Stripping Distribution Coefficient p and q with ELM Experiments and Analytical Solution of the Mathematical Model

4.4.1 Experimental

The ELM experiments are performed to evaluate the extraction and stripping distribution coefficients. The external phase is the cadmium ion solution which is prepared by dissolving cadmium sulfate (Sigma) in DI water. The pH is adjusted by the sodium acetate- acetic acid buffer. The emulsion consists of the membrane phase and the internal phase. The membrane phase contains diluent, Exxol-D80, carrier, D2EHPA and surfactant, ECA4360J. ECA4360J is a nonionic polyamine with a molecular weight of about 1800 manufactured at Exxon. It can prevent swelling of the system and stabilize the emulsion (18, 65, 66, 67). A typical volume fraction of three components is 88:10:2. First, 5% extractant E2EHPA and 3% surfactant ECA4360J are added to the diluent, Exxol-D80. Then the internal phase which is 3M H_2SO_4 is poured into the formulated membrane phase at a ratio of 1/9. The solution is emulsified by Warring Commercial Laboratory Blender for 25 minutes at the fixed speed of 10,000rpm. After that, the emulsion is cooled down to room temperature and is ready for the experiment. The emulsion is freshly prepared each time before the permeation experiment.

The prepared emulsion is then dispersed into an agitated vessel with the external solution in a volume ration of 1/5. The agitator speed is controlled at 300 rpm to 350rpm by a G.K.Heller Corporation, GT-21 motor controller and detected by a laser detector. Samples are taken every couple minutes during agitation. After 30 minutes, the agitation is stopped. The samples are placed into the VWR Scientific GT-2 centrifuges for 10 minutes to ensure the complete separation of the external phase and the emulsion phase.

Then the sample's aqueous phase is pipetted, diluted and ready for instrumental analysis. A flame atomic absorption spectrophotometer is used to analyze the cadmium ion concentrations in the samples at the wavelength of 228.8nm (29).

4.4.2 Evaluate Extraction and Stripping Distribution Coefficients p and q

The ELM experiments give data of the external concentration profile, which is the metal ion concentration versus time. The model that was developed in Chapter 2 gives the theoretical prediction of the concentration profile. Hence, the parameters, p and q can be evaluated with the experimental data.

The concentration profile obtained from the analytical solution which is given in Chapter 2, section 2.2, is:

$$\frac{C_e}{C_{e0}} = \frac{3}{B+3} + \sum_{n=1}^{\infty} \frac{2B}{3B + B^2 + b_n^2 + Gb_n^2(Gb_n^2 - 2B - 1)} \exp(-\frac{b_n^2}{\omega}\tau) \qquad (2.24)$$

As t goes to infinity, the theoretical value is:

$$\frac{C_{e\infty}}{C_{e0}} = \frac{3}{B+3} = \frac{V_e}{V_e + p(V_m + qV_i)} \qquad (2.32)$$

The procedure to find p and q is:

1. Read the value of $C_{e\infty}/C_{e0}$ from experimental curve when t=∞
2. From equation (2.32) obtain q = f (p)
3. From the analytical solution of C_e/C_{e0} versus t with p and q as the parameters, find the best value of p and q that gives the closest fit to the experimental data.

A suite of Visual Basic Applications has been developed to numerically calculate the solutions. For given values of p and q, the programs compute the theoretical external concentration profile and compare it with the experimental external concentration profile. Thus, the values of p and q can be found that produces the best fit by minimizing the standard error.

4.4.2.1 Calculation of Parameter: Chemical and physical parameters are needed as input into the program. Published correlations can be used to evaluate the parameters and then placed into the program. One set of ELM experimental data for cadmium ion can be used as an example (Figure 4.3). The experimental condition is: Membrane phase contains 5% D2EHPA, 7% ECA 4360 and 88% D-80, internal phase contains 3M H_2SO_4 and external phase is 938ppm Cd^{2+} with pH=2.91. The experimental curve shows the external concentration as a function of time.

1. Evaluate Effective Diffusivity of metal-carrier complex in emulsion phase D_e

The diffusivity of cadmium sulfate in the aqueous phase D_i and the diffusivity of the cadmium-D2EHPA complex in membrane phase D_m are evaluated by the Wilke-Chang equation (68).

The Wilke-Chang equation is:

$$D_i = \frac{7.4 * 10^{-12} (\phi * M_B)^{1/2} T}{\eta_B V_A^{0.6}} (m^2 / \text{sec}) \qquad (4.13)$$

Where: ϕ= Associate factor of solvent (2.6 for water, 1.0 for unassociated solvent)

M_B= Molecular weight of solvent phase (g/mol)

T= Absolute temperature (K)

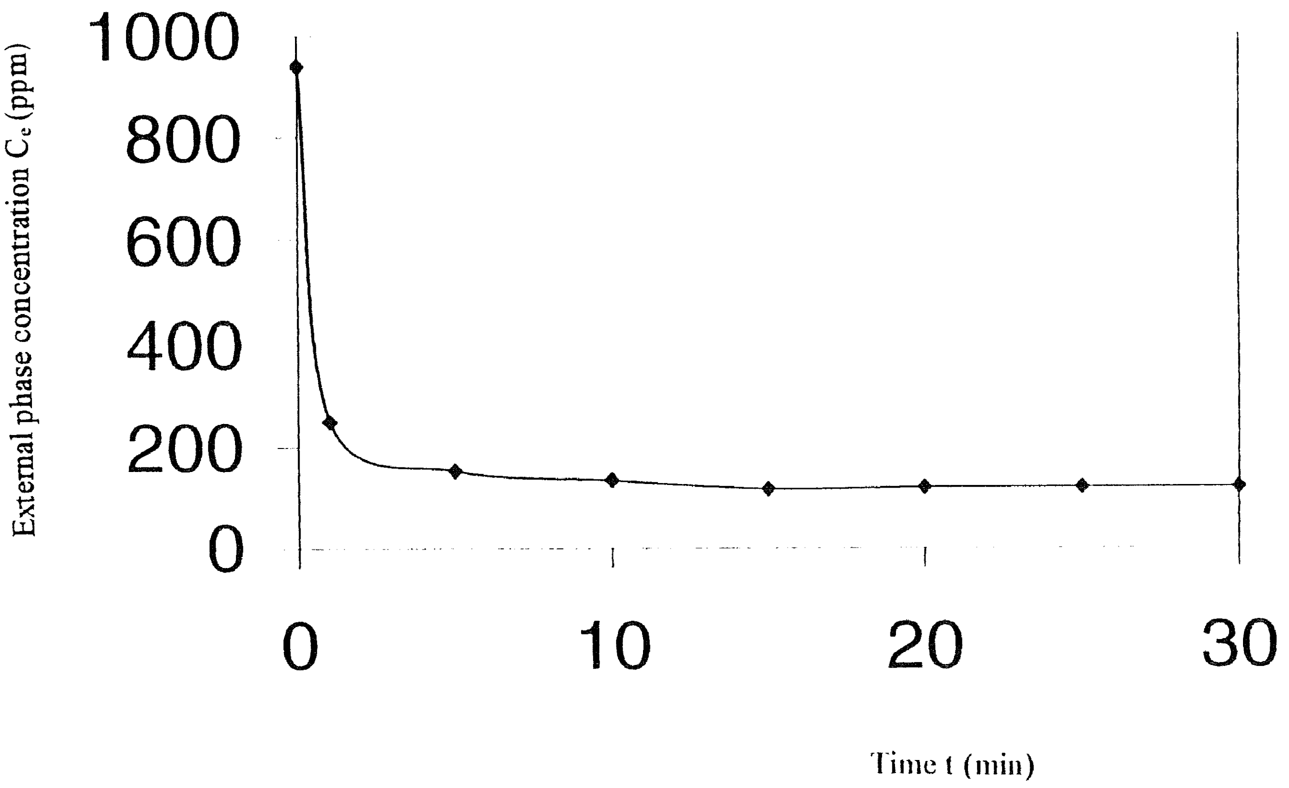

Figure 4.3 External Phase Concentration Profile of an ELM Experiment

η_B= Viscosity of solvent phase (cp)

V_A= Molar volume of solute A at its normal boiling temperature (cm^3/mol)

Table 4.1 Molar volume of some elements for the determination of the molar volume of cadmium complex at its normal boiling temperature (Le Bas correlation)

Elements	Carbon C	Hydrogen H	Oxygen O	Cadmium	sulfur
V_A(cm^3/mol)	5.29	3.7	12	14	16

Assume that the molar volume of Phosphorus is 10.

The molar volume of solute V_A is calculated by the Le Bas correlation (69).

For $CdSO_4$ in aqueous phase:

V_A=14+16+4*12=78(cm^3/mol)

The associate factor of the solvent ϕ=2.6 (for the aqueous phase);

The molecular weight of the aqueous phase, M_B=18 (g/mol);

The absolute temperature, T=298.15 (K);

The viscosity of aqueous phase, η_B=1.0 (cp);

The above data are placed into Wilke-Chang equation, and the diffusivity of $CdSO_4$ in aqueous phase is obtained:

$$D_i = \frac{7.4 \times 10^{-12} (\phi \times M_B)^{1/2} T}{\eta_B V_A^{0.6}} (m^2 / \sec) = 1.105 \times 10^{-9} (m^2 / s)$$

For $CdR_2 \bullet 3RH$ complex in the membrane phase:

The $CdR_2 \bullet 3RH$ is equivalent to $C_{16}H_{34}O_4PCd$, therefore, the molar volume of $CdR_2 \bullet 3RH$ is:

$V_A = 16*5.29+34*3.7+4*12+10+14 = 282.44$ (cm^3/mol)

The associate factor of the solvent $\phi = 1.0$ (for the organic phase);

The molecular weight of the membrane phase diluent Exxol D-80, $M_B = 177$ (g/mol);

The absolute temperature, $T = 298.15$ (K);

The viscosity of aqueous phase, $\eta_B = 1.7$ (cp);

The above data are placed into the Wilke-Chang equation, and the diffusivity of $CdR_2 \bullet 3RH$ in the organic phase is obtained:

$$D_m = \frac{7.4 \times 10^{-12} (\phi \times M_B)^{1/2} T}{\eta_B V_A^{0.6}} (m^2 / \sec) = 5.83 \times 10^{-10} (m^2 / s)$$

The Jefferson-Witzell-Sibbert correlation is used to calculate the effective diffusivity of the complex in the membrane phase (70):

$$D_e = D_m \left(\frac{4(1+2h)^2 - \pi}{4(1+2h)^2}\right) + \frac{\pi}{4(1+2h)^2} \left(\frac{(1+2h) D_A D_m}{D_m + 2h D_A}\right) \qquad (4.14)$$

where

$$D_A = \frac{2(\frac{D_i}{p})D_m}{\frac{D_i}{p}-D_m}[\frac{\frac{D_i}{p}}{\frac{D_i}{p}-D_m}\ln(\frac{\frac{D_i}{p}}{D_m})-1]$$

$$h = 0.403(\frac{V_i}{V_m+V_i})^{-\frac{1}{3}}-0.5$$

Diffusivity of Cadmium sulfate in aqueous phase D_i and diffusivity of cadmium-D2EHPA complex in membrane phase D_m are determined above;

The internal phase volume V_i = 9ml;

The membrane phase volume V_m =41ml.

The extraction distribution coefficient is p=24(determined from single stage equilibrium experiment).

The above data are placed into Jefferson-Witzell-Sibbert correlation, and the effective diffusivity, D_e=4.06*10^{-10} (m^2/sec). The effective diffusivity represents the diffusivity of Cd-D2EHPA complex in the membrane phase. It is less than the diffusivity of the complex in the organic phase, D_m, because of the block by the internal aqueous droplets. The effective diffusivity also may increase when the internal volume ratio ($V_i/(V_i+V_m)$) increases.

2. Evaluation of the External Mass Transfer Coefficient, k

The external mass transfer coefficient, k, is determined by Skelland & Lee equation (71):

$$\frac{k}{\sqrt{ND_i}} = 2.932*10^{-7}\left(\frac{V_i+V_m}{V_i+V_m+V_e}\right)^{-0.508}\left(\frac{d_I}{d_T}\right)^{0.548}\mathrm{Re}^{1.371}$$

$$\mathrm{Re} = \frac{Nd_I^2\rho}{\mu} \qquad (4.15)$$

Table 4-2 Variables and their assigned data in determining the external mass transfer coefficient of cadmium system

N: agitating speed(rps)	5
D_I: external diffusivity(m^2/sec)	$1.11*10^{-9}$
d_I: diameter of the propeller(m)	0.04
d_T: diameter of the tank(m)	0.1
V_i: volume of internal phase(ml)	9
V_m: volume of membrane phase(ml)	41
V_e: volume of external phase(ml)	500
ρ: density of the external phase(g/cm^3)	1.0
μ: viscosity of the external phase(g/cm/sec)	0.01

The above data are placed into Skelland & Lee equation and yields the Reynold number, $Re=8*10^3$ and the external mass transfer coefficient, $k=1*10^{-5}$ (m/sec).

3. Evaluation of Sauter mean globule radius

The Sauter mean radius of the emulsion globules is determined by the same method as Ohtake (41).

When the viscosity of the emulsion phase η <160cp,

$$\frac{d_{32}}{d_I} = 0.12 W_e^{-0.5} \tag{4.16}$$

When viscosity of emulsion phase η >160cp,

$$\frac{d_{32}}{d_I} = 0.5 \eta^{0.8} W_e^{-0.5} \tag{4.17}$$

Where d_{32}=the Sauter mean diameter (cm)

Table 4.3 Variables and their assigned data for determination of sauter mean diameter

N: agitation speed(rps)	5
D_I: diameter of the propeller(m)	0.04
ρ: density of the external phase(g/cm)	1.0
γ: surfacial tension	72.8

Since the viscosity of the emulsion is less than 160cp for the ELM systems, the first Ohtake equation is used. The above data are placed into the first Ohtake Equation, and the Sauter mean diameter, d_{32}=0.116(cm)

4.4.2.2 Find the Best Extraction and Stripping Distribution Coefficients with the Computer Program: All of the above parameters are placed into the computer program that was developed. The experimental data which are the external metal ion concentrations as a function of time were also entered into the computer program. The best extraction and stripping distribution coefficients p and q are found by minimizing the standard errors. With this set of ELM experimental data, an extraction distribution coefficient, p, is in the range from 18 to 40 and those values give minimized standard error. However, stripping distribution coefficient q can be in a very wide range from 10^3 to 10^6 to give the smallest standard error.

4.5 Compare the Theoretical Values of Extraction Distribution Coefficient and Stripping Distribution Coefficient with Experimental Values

The extraction and stripping distribution coefficients can be compared with predicted values from the theoretical prediction. Theoretically, the extraction distribution coefficient can be calculated by:

$$p = K \frac{[RH]_m^{2.5}}{K_\gamma [H^+]_m^2} \tag{4.18}$$

As the organic phase nonideality is neglected, equation (4.18) becomes:

$$p = K\frac{[RH]_n^{2.5}\gamma_{Cd^{2+}}^2}{[H^+]_n^2\gamma_{H^+}^2} \tag{4.19}$$

The Davies modified extended Debye-Huckel model is used to calculate the activity coefficient: $\log\gamma_i = -Az_i^2(\frac{I^{0.5}}{1+I^{0.5}} - 0.3I)$ (3.13)

where I = the ionic strength of solution

$$I = \tfrac{1}{2}\sum_{i=1}^{n} c_i z_i^2 \tag{3.16}$$

z_i = the ionic charge; c_i = the concentration of ionic species; A =0.509;

At equilibrium, the concentrations are [Cd^{2+}]=131ppm=0.001165mol/l and [H^+]=$10^{-2.91}$=0.00123mol/l. These data are placed into equations (3.16) and (3.15), and

$$I = \tfrac{1}{2}\sum_{i=1}^{n} c_i z_i^2 = \tfrac{1}{2}(0.001165\times 2^2 + 0.00123\times 1) = 0.00295$$

and

$$\log\gamma_{Cd^{2+}} = -Az_i^2\frac{I^{0.5}}{1+I^{0.5}} + BI = -0.509\times 2^2\left(\frac{0.00295^{0.5}}{1+0.00295^{0.5}} - 0.3\times 0.00295\right)$$
$$= -0.103084$$

or,

$$\gamma_{Cd^{2+}} = 0.788707$$

$$\log\gamma_{H^+} = -Az_i^2\frac{I^{0.5}}{1+I^{0.5}} + BI = -0.509\times 1^2\left(\frac{0.00295^{0.5}}{1+0.00295^{0.5}} - 0.15\times 0.00295\right)$$
$$= -0.02532$$

hence,

$$\gamma_{H^+} = 0.943$$

At equilibrium, the extractant concentration is approximately the initial concentration because most of the metal ion is released and the extractant becomes free. The volume of D2EHPA is 5%. The molecular weight of D2EHPA is 322.4g/mol. The density of D2EHPA is 0.98g/cm. The initial D2EHPA concentration is 0.152mol/l. The concentration of the dimer D2EHPA $[(RH)_2]$=0.152/2=0.076mol/l. At equilibrium the pH value is 2.91 which means the concentration of hydrogen ion $[H+]=10^{-2.91}$=0.00123mol/l.

As previously shown, the equilibrium constant for the interfacial reaction is K=0.0258.

The above data are all placed into equation(4.19) and

$$p = K\frac{[RH]_m^{2.5}\gamma^2_{Cd^{2+}}}{[H^+]_m^2\gamma^2_{H^+}} = 0.0258\times\frac{0.076^{2.5}}{0.00123^2}\times\frac{0.789}{0.942^2} = 24$$

The extraction distribution coefficient obtained from the theory, 24, is consistent with the value obtained from the ELM experiment, 18 to 40. Hence, the value of extraction distribution coefficient can be determined without running experiments.

The extraction distribution coefficient obtained from single-stage equilibrium data is compared with data from the above two methods and the values are close. Since data at a pH=2.91 are not available, the curve in Figure 4.2 is used to find the value at a pH=2.91, and the extraction efficiency is about 95%. With the definition of extraction distribution coefficient, the value of p=19. This range is very close to the theoretical prediction. This further proves the theory that has been developed.

The stripping distribution coefficient can be theoretically calculated by equation (4.20)

$$q = \frac{[H^+]_i^2}{K_\gamma [RH]_m^{2.5}} \{K_1 + K_1 K_2 [SO_4^{2-}]_i\} \tag{4.20}$$

Since the organic phase activity coefficients are one, therefore:

$$q = \frac{\gamma_{H_i^+}^2 [H^+]_i^2}{\gamma_{Cd_i^{2+}} [(RH)_2]_m^{2.5}} \{K_1 + K_1 K_2 [SO_4^{2-}]_i\} \tag{4.21}$$

The internal phase concentration of H_2SO_4 is 3M and the hydrogen ion concentration can be approximated as $[H^+]$=3mol/l. The extractant concentration $[(RH)_2]$=0.152/2=0.076mol/l.

The extended Debye-Huckel model is used to calculate the activity coefficient. First the the ionic strength is:

$I = \frac{1}{2}\sum_{i=1}^{n} c_i z_i^2 \approx \frac{1}{2}(3 \times 1^2) = 1.5$(Ignore the term for the metal ion as it is very small compare to the term of the hydrogen ion)

Since the extended Debye-Huckel model is for ionic strength less than 0.1, this model can not be used for an ionic strength equal to 1.5. Other methods are investigated in order to get the activity coefficients at higher concentrations. Finally, activity coefficients at these concentrations are found to be γ_H^+=0.119 and γ_{Cd}^+=0.517 respectively (72).

The equilibrium constant of the membrane-internal interfacial reaction K_1 is the reciprocal of the equilibrium constant of external-membrane interfacial reaction K.

$$K_1 = \frac{1}{K} = \frac{1}{0.0258} = 38.16$$

The equilibrium constant of the internal phase reaction, K_2 is 281.8 (63).

The above data are placed into equation (4.21) and the stripping distribution coefficient is $q=1.38*10^6$. Using this value in the computer program gives the smallest standard error. This shows that the stripping distribution coefficient can also be predicted by the theory that was developed without running an ELM experiment.

The stripping distribution coefficient can be calculated without considering the internal phase reaction which means that the second term in equation (4.21) is zero. Thus the stripping distribution coefficient is:

$$q = \frac{\gamma_{H_i^+}^2 \left[H^+\right]_i^2}{\gamma_{Cd_i^{2+}} \left[(RH)_2\right]_m^{2.5}} K_1 \tag{4.22}$$

The data which were obtained are placed into this equation and q=3938. This value of q is entered into the computer program and it also gives the smallest standard error. This shows that the stripping distribution coefficient is large enough to transfer the metal ion into the internal phase. To increase the value from 10^3 to a larger value does not have a dramatic impact on the performance of ELM system.

To further verify the theory on the extraction distribution coefficient, data on page 168 of K. C. Wang's thesis (52) are used. Wang did copper ion extraction with LIX-64N as extractant and HNO_3 as internal phase.

Since the organic phase activity coefficients are near one, the extraction distribution coefficient can be written as:

$$p = K\frac{[RH]_m^2}{K_\gamma [H^+]_e^2} = K\frac{[RH]_m^2 \gamma_{Cu^{2+}}}{[H^+]_e^2 \gamma_{H^+}^2} \tag{4.23}$$

At equilibrium, the copper ion concentration $[Cu^{2+}]$=26.4ppm=0.000384mol/l and hydrogen ion concentration $[H^+]=10^{-2.3}$=0.00501mol/l. The ionic strength is:

$$I = \tfrac{1}{2}\sum_{i=1}^{n} c_i z_i^2 = \tfrac{1}{2}(0.000384 \times 2^2 + 0.00501 \times 1) = 0.003275$$

then, $\log \gamma_{Cu^{2+}} = -Az_i^2 \dfrac{I^{0.5}}{1+I^{0.5}} + BI = -0.10823$

$$\gamma_{Cu^{2+}} = 0.779$$

$$\gamma_{H^+} = 0.9396$$

Wang's thesis gives:

$$K[RH]_m^2 = 1.27 \times 10^{-5}$$

These data are placed into equation (4.23), and the extraction distribution coefficient is p=0.446.

Wang's thesis states the value of the extraction distribution coefficient, p, is 0.402 which is very close to the theoretical prediction 0.446.

The same set of data given by Wang is put into the computer program. The results show that the best value of extraction distribution coefficient, p, is from 0.40 to 0.43. This range is also very close to the theoretical value 0.446.

It can be concluded that the extraction distribution coefficient, p, and stripping distribution coefficient, q, can be theoretically predicted with equations (3.22) and (3.28) (extraction of copper ion is used as an example to illustrate the method).

$$p = K\frac{[RH]_m^2}{K_\gamma [H^+]_e^2} \tag{3.22}$$

$$q = \frac{[H^+]_i^2}{K_\gamma' [RH]_m^2}\{K_1 + K_1 K_2 [SO_4^{2-}]_i\} \tag{3.28}$$

4.6 Discussion

The concentration profile obtained in Chapter 2, section 2.2, is

$$\frac{C_e}{C_{e0}} = \frac{3}{B+3} + \sum_{n=1}^{\infty} \frac{2B}{3B + B^2 + b_n^2 + Gb_n^2(Gb_n^2 - 2B - 1)} \exp(-\frac{b_n^2}{\omega}\tau) \tag{2.24}$$

As t goes to infinity, the theoretical value is:

$$\frac{C_{e\infty}}{C_{e0}} = \frac{3}{B+3} \tag{2.32}$$

where: $B=pf'\omega$

$$\omega = 1 - e + e(1 + K_2 [SO_4^{2-}]_i)q \tag{3.33}$$

Therefore, when time goes to infinity, the system reaches equilibrium. At equilibrium, the external metal ion concentration is $3C_{e0}/(B+3)$.

At equilibrium, the recovery efficiency $E(\infty) = 1 - \frac{C_{e\infty}}{C_{e0}} = \frac{B}{B+3}$ (2.33)

Equation (2.33) is the best performance an ELM system can achieve. This means that no matter how hard one tries, the highest recovery efficiency for this system can not be larger than B/(B+3), and B/(B+3) is the maximum recovery efficiency for an ELM system. Equation (2.33) also shows that a larger value of B gives a larger maximum recovery efficiency. Therefore B should be as high as possible.

For equation (3.33), when the term $K_2[SO_4^{2-}]$ is much larger than 1 and usually it is, the terms of 1, e (e<1), and eq can be neglected, and equation (3.37) becomes:

$$\omega \approx K_2\left[SO_4^{2-}\right]_i qe \tag{4.24}$$

Hence, $B \approx K_2\left[SO_4^{2-}\right]_i f' pqe$ (4.25)

Equation (4.25) shows that increasing p and q will give larger values of B and a higher recovery efficiency at equilibrium. Since the extraction distribution coefficient

$p = K\frac{[RH]_m^2}{K_\gamma [H^+]_e^2}$ and stripping distribution coefficient

$q = \frac{[H^+]_i^2}{K_\gamma' [RH]_m^2}\{K_1 + K_1K_2\left[SO_4^{2-}\right]_i\}$, therefore,

$$B = K_2\left[SO_4^{2-}\right]_i f' pqe = \frac{[H^+]_i^2}{[H^+]_e^2} f' e \frac{K}{K_\gamma K_\gamma'} K_2\left[SO_4^{2-}\right]_i \{K_1 + K_1K_2\left[SO_4^{2-}\right]_i\} \tag{4.26}$$

Equation (4.26) shows that to achieve better performance, the internal phase hydrogen ion concentration should increase and the external hydrogen ion concentration should be decreased. Equation (4.26) also gives other factors that affect the performance of the ELM system. A larger ratio of the emulsion to the external phase gives better performance. However, the volume ratio can not be selected arbitrarily because of the stability of the emulsion. Larger equilibrium constants for interfacial reactions and internal phase reaction give a larger recovery efficiency. These observations mean that a good selection of the extractant and internal phase acid with bigger reaction rate constants will enhance the performance of ELM. Larger acid concentrations in the internal phase will also enhance the efficiency. Equation (4.26) gives very valuable guidance for the operation of ELM experiments.

If no terms in the equation $\omega = 1 - e + e(1 + K_2[SO_4^{2-}]_i)q$ are neglected, then,

$$\begin{aligned} B &= pf'\omega = pf'\{1 - e + e(1 + K_2[SO_4^{2-}]_i)q\} \\ &= pf'(1-e) + pf'qe(1 + K_2[SO_4^{2-}]_i) \\ &= K\frac{[RH]_m^2}{K_\gamma [H^+]_e^2} f'(1-e) + \frac{[H^+]_i^2}{[H^+]_e^2} f'e\frac{K}{K_\gamma K_\gamma'}(1 + K_2[SO_4^{2-}]_i)\{K_1 + K_1K_2[SO_4^{2-}]\} \end{aligned}$$

(4.27)

Equation (4.27) shows that the extractant concentration does affect the first term of B. Hence, a larger extractant concentration will give a larger value of B and then better performance. However, in many cases, the first term is much smaller than the second one and the impact of extractant concentration on the equilibrium recovery efficiency is not significant. Equation (4.27) also shows that the internal phase volume fraction of emulsion, e, has impact on the recovery efficiency. However, we can not change the fraction too much because of the stability of the emulsion.

CHAPTER 5

CONCLUSION

5.1 Conclusion

It can be concluded that the experimentally measured values of the extraction distribution coefficient p and stripping distribution coefficient q are no longer necessary. The extraction and stripping distribution coefficients can be predicted theoretically. Thus with the mathematical modeling of the ELM, the concentration profile can be predicted without running an ELM experiments. The best recovery efficiency can be predicted theoretically. This study gives the theoretical guidance to find the optimal experimental operating conditions.

The impact of the internal reaction on the external phase concentration profile exists. However, within the experimental time period, the difference between the model considering internal phase reaction and the model not considering the internal phase reaction is not significant. The impact of the internal phase reaction on equilibrium external concentration is, however, noticeable.

A singularity in the eigenvalue equation is found which was neglected in previous studies. Thus the second eigenvalue is located which has an important impact in the concentration profiles.

5.2 Recommendation

This thesis ignored the nonideality of the organic phase of ELM which might result in some deviation on the equilibrium constant. Further studies may include the study of the activities of the organic phase of the ELM system.

APPENDIX

COMPUTER CODE

```
Option Explicit

' This function computes the dimensionless external concentration
ConcentrationRatio=Ce/Ce0

Function ConcentrationRatio(ByVal G As Double, ByVal B As Double, _
        ByVal t As Double) As Double
   Dim ratio As Double, n As Integer, abv As Double, increment As Double
   Dim num_roots As Integer, root As Double, brac As Double, pi As Double
   Dim start_bn As Double, end_bn As Double, coef As Double
   Dim increment1 As Double, increment2 As Double
   Dim ratio0 As Double

   pi = 3.1415926
   ratio0 = 3 / (B + 3)
   ratio = ratio0

   For n = 1 To 10000
      num_roots = NumRoots(G, B, n)
      If (num_roots = 1) Then
         start_bn = (n - 1 / 2) * pi
         end_bn = (n + 1 / 2) * pi
         root = FindRoot(G, B, start_bn, end_bn)
         coef = CeCoef(G, B, root)
         increment = coef * Exp(-root * root * t)
         abv = Abs(increment)
      Else
         brac = FindBrac(G, B, n)
         start_bn = (n - 1 / 2) * pi
         end_bn = brac
         root = FindRoot(G, B, start_bn, end_bn)
         coef = CeCoef(G, B, root)
         increment1 = coef * Exp(-root * root * t)
         start_bn = brac
         end_bn = (n + 1 / 2) * pi
         root = FindRoot(G, B, start_bn, end_bn)
         coef = CeCoef(G, B, root)
         increment2 = coef * Exp(-root * root * t)
         increment = increment1 + increment2
         abv = Abs(increment2)
      End If
```

```
        ratio = ratio + increment
        If abv < Abs(ratio0) * 0.0001 Then
           Exit For
        End If

    Next n

    ConcentrationRatio = ratio

End Function


' This function computes the dimensionless external concentration
' ConcentrationRatio=Ce/Ce0 given p, w (Omega), f, De, R, k, t
' where t is the real time (RT)
' t1 is the dimentionless time tao/w.

Function ConcentrationRatioRT(ByVal p As Double, ByVal w As Double, _
            ByVal f As Double, ByVal De As Double, _
            ByVal R As Double, ByVal k As Double, _
            ByVal t As Double) As Double

    Dim B As Double, G As Double, t1 As Double

    B = p * f * w
    G = p * De / (R * k)
    t1 = De * t / (w * R ^ 2)

    ConcentrationRatioRT = ConcentrationRatio(G, B, t1)

End Function

' This function computes the dimensionless external concentration
ConcentrationRatio=Ce/Ce0
' But it ignores one of the two eigenvalues around the singular point
' when G>1

Function ConcentrationRatioWrong(ByVal G As Double, ByVal B As Double, _
           ByVal t As Double) As Double
    Dim ratio As Double, n As Integer, abv As Double, increment As Double
    Dim num_roots As Integer, root As Double, brac As Double, pi As Double
    Dim start_bn As Double, end_bn As Double, coef As Double
    Dim increment1 As Double, increment2 As Double
    Dim ratio0 As Double

    pi = 3.1415926
```

```
  ratio0 = 3 / (B + 3)
  ratio = ratio0

  For n = 1 To 10000
    num_roots = NumRoots(G, B, n)
    If (num_roots = 1) Then
      start_bn = (n - 1 / 2) * pi
      end_bn = (n + 1 / 2) * pi
      root = FindRoot(G, B, start_bn, end_bn)
      coef = CeCoef(G, B, root)
      increment = coef * Exp(-root * root * t)
      abv = Abs(increment)
    Else
      brac = FindBrac(G, B, n)
      start_bn = (n - 1 / 2) * pi
      end_bn = brac
      root = FindRoot(G, B, start_bn, end_bn)
      coef = CeCoef(G, B, root)
      increment1 = coef * Exp(-root * root * t)
      start_bn = brac
      end_bn = (n + 1 / 2) * pi
      root = FindRoot(G, B, start_bn, end_bn)
      coef = CeCoef(G, B, root)
      increment2 = coef * Exp(-root * root * t)
      increment = increment1
      abv = Abs(increment2)
    End If

    ratio = ratio + increment
    If abv < Abs(ratio0) * 0.0001 Then
      Exit For
    End If

  Next n

  ConcentrationRatioWrong = ratio

End Function

' The coefficient in external Concentration Ce/Ce0
Function CeCoef(ByVal G As Double, ByVal B As Double, _
            ByVal bn As Double) As Double
  CeCoef = 2 * B / (3 * B + B ^ 2 + bn ^ 2 + G * (bn ^ 2) * (G * (bn ^ 2) - 2 * B - 1))

End Function
```

```
Option Explicit

Function RHS(ByVal G As Double, ByVal B As Double, _
        ByVal bn As Double) As Double
   Dim diff As Double
   diff = B - G * bn ^ 2
   RHS = diff * bn / (diff + bn ^ 2)

End Function


Function fun_0(ByVal G As Double, ByVal B As Double, _
        ByVal bn As Double) As Double
   Dim Coef1 As Double, Coef2 As Double

   Coef1 = B - (G - 1) * bn ^ 2
   Coef2 = B - G * bn ^ 2
   fun_0 = (Coef1 * Sin(bn) - Coef2 * bn * Cos(bn)) / B

End Function

Function fun_1(ByVal G As Double, ByVal B As Double, _
        ByVal bn As Double) As Double
   Dim Coef1 As Double, Coef2 As Double

   Coef1 = (B - 2 * G + 2) * bn - G * (bn ^ 3)
   Coef2 = (2 * G + 1) * (bn ^ 2)
   fun_1 = (Coef1 * Sin(bn) + Coef2 * Cos(bn)) / B

End Function

Function fun_2(ByVal G As Double, ByVal B As Double, _
        ByVal bn As Double) As Double
   Dim Coef1 As Double, Coef2 As Double

   Coef1 = (B - 2 * G + 2) - (5 * G + 1) * (bn ^ 2)
   Coef2 = (B + 2 * G + 4) * bn - G * (bn ^ 3)
   fun_2 = (Coef1 * Sin(bn) + Coef2 * Cos(bn)) / B

End Function

' Find the number of roots between (n-1/2)*pi and (n+1/2)*pi

Function NumRoots(ByVal G As Double, ByVal B As Double, _
           ByVal n As Integer) As Integer
```

```
 Dim num As Integer, pi As Double
 Dim start_bn As Double, end_bn As Double
 Dim start_val As Double, end_val As Double

 pi = 3.1415926
 start_bn = (n - 1 / 2) * pi
 end_bn = (n + 1 / 2) * pi

 start_val = fun_0(G, B, start_bn)
 end_val = fun_0(G, B, end_bn)

 If (start_val * end_val > 0) Then
    num = 2
 Else
    num = 1
 End If

 NumRoots = num

End Function

'The function FindRoot finds the root for fun_0 using bisection
' between start_bn and end_bn if there is only one root in
' the interval between start_bn and end_bn

Function FindRoot(ByVal G As Double, ByVal B As Double, _
            ByVal start_bn As Double, ByVal end_bn As Double) As Double
  Dim left As Double, right As Double, mid As Double
  Dim left_val As Double, right_val As Double, mid_val As Double
  Dim n As Integer

  left = start_bn
  right = end_bn
  mid = 0.5 * (left + right)

  left_val = fun_0(G, B, left)
  right_val = fun_0(G, B, right)
  mid_val = fun_0(G, B, mid)
  n = 0

  Do While ((Abs(mid_val) > 0.00001) And (n < 10000))
     If (left_val * mid_val > 0) Then
        left = mid
        left_val = mid_val
     Else
        right = mid
```

```
      End If
      mid = 0.5 * (left + right)
      mid_val = fun_0(G, B, mid)
      n = n + 1
   Loop

   FindRoot = mid
End Function

' If there are two roots between (n-1/2)*pi and (n+1/2)*pi
' The function FindBrac finds a point between them so
' there is one root on each side of the point
Function FindBrac(ByVal G As Double, ByVal B As Double, _
            ByVal n As Integer) As Double
   Dim m As Integer
   Dim interval As Double, pi As Double
   Dim left As Double, brac As Double, right As Double
   Dim left_val As Double, brac_val As Double
   Dim prod As Double
   pi = 3.1415926

   left = (n - 1 / 2) * pi
   right = (n + 1 / 2) * pi

   left_val = fun_0(G, B, left)

   For m = 1 To 10
      interval = pi / (2 ^ m)
      brac = left + interval
      Do While (brac < right)
         brac_val = fun_0(G, B, brac)
         prod = brac_val * left_val
         If (prod < 0) Then
            Exit For
         End If
         brac = brac + interval
      Loop
   Next m

   FindBrac = brac

End Function

Sub FR()
'   Cells(10, 1).Value = FindRoot(11, 400, 1.5 * 3.1415926, 2 * 3.1415926) / 3.1415926
   Cells(30, 1).Value = FindBrac(11, 400, 2)
```

```
End Sub

Option Explicit

' This function computes the dimensionless
' concentration CR_IM=Ce*/Ce0 at the external membrane
' interface

Function CR_IM(ByVal G As Double, ByVal B As Double, _
        ByVal t As Double) As Double
   Dim ratio As Double, n As Integer, abv As Double, increment As Double
   Dim num_roots As Integer, root As Double, brac As Double, pi As Double
   Dim start_bn As Double, end_bn As Double, coef As Double
   Dim increment1 As Double, increment2 As Double
   Dim ratio0 As Double

   pi = 3.1415926
   ratio0 = 3 / (B + 3)
   ratio = ratio0

   For n = 1 To 10000
      num_roots = NumRoots(G, B, n)
      If (num_roots = 1) Then
         start_bn = (n - 1 / 2) * pi
         end_bn = (n + 1 / 2) * pi
         root = FindRoot(G, B, start_bn, end_bn)
         coef = CeIMCoef(G, B, root)
         increment = coef * Exp(-root * root * t)
         abv = Abs(increment)
      Else
         brac = FindBrac(G, B, n)
         start_bn = (n - 1 / 2) * pi
         end_bn = brac
         root = FindRoot(G, B, start_bn, end_bn)
         coef = CeIMCoef(G, B, root)
         increment1 = coef * Exp(-root * root * t)
         start_bn = brac
         end_bn = (n + 1 / 2) * pi
         root = FindRoot(G, B, start_bn, end_bn)
         coef = CeIMCoef(G, B, root)
         increment2 = coef * Exp(-root * root * t)
         increment = increment1 + increment2
         abv = Abs(increment2)
      End If

      ratio = ratio + increment
```

```
    If abv < Abs(ratio0) * 0.0001 Then
      Exit For
    End If

  Next n

  CR_IM = ratio
End Function

' This function computes the dimensionless
' concentration CR_IM=Ce*/Ce0 at the external membrane
' interface given p, w (Omega), f', De, R, k, t where t is the
' real time (RT)
' t1 is the dimentionless time tao/w.

Function CR_IMRT(ByVal p As Double, ByVal w As Double, _
        ByVal f As Double, ByVal De As Double, _
        ByVal R As Double, ByVal k As Double, _
        ByVal t As Double) As Double

  Dim B As Double, G As Double, t1 As Double

  B = p * f * w
  G = p * De / (R * k)
  t1 = De * t / (w * R ^ 2)

  CR_IMRT = CR_IM(G, B, t1)

End Function


' This function computes the dimensionless
' concentration CR_IM=Ce*/Ce0 at the external membrane
' interface

Function CR_IMWrong(ByVal G As Double, ByVal B As Double, _
        ByVal t As Double) As Double
  Dim ratio As Double, n As Integer, abv As Double, increment As Double
  Dim num_roots As Integer, root As Double, brac As Double, pi As Double
  Dim start_bn As Double, end_bn As Double, coef As Double
  Dim increment1 As Double, increment2 As Double
  Dim ratio0 As Double

  pi = 3.1415926
  ratio0 = 3 / (B + 3)
  ratio = ratio0
```

```
  For n = 1 To 10000
    num_roots = NumRoots(G, B, n)
    If (num_roots = 1) Then
      start_bn = (n - 1 / 2) * pi
      end_bn = (n + 1 / 2) * pi
      root = FindRoot(G, B, start_bn, end_bn)
      coef = CeIMCoef(G, B, root)
      increment = coef * Exp(-root * root * t)
      abv = Abs(increment)
    Else
      brac = FindBrac(G, B, n)
      start_bn = (n - 1 / 2) * pi
      end_bn = brac
      root = FindRoot(G, B, start_bn, end_bn)
      coef = CeIMCoef(G, B, root)
      increment1 = coef * Exp(-root * root * t)
      start_bn = brac
      end_bn = (n + 1 / 2) * pi
      root = FindRoot(G, B, start_bn, end_bn)
      coef = CeIMCoef(G, B, root)
      increment2 = coef * Exp(-root * root * t)
      increment = increment1
      abv = Abs(increment2)
    End If

    ratio = ratio + increment
    If abv < Abs(ratio0) * 0.0001 Then
      Exit For
    End If

  Next n

  CR_IMWrong = ratio
End Function



' The coefficient in Concentration Ce*/Ce0
' at the external membrane interface

Function CeIMCoef(ByVal G As Double, ByVal B As Double, _
          ByVal bn As Double) As Double
  CeIMCoef = 2 * (B - G * bn ^ 2) / (3 * B + B ^ 2 + bn ^ 2 + G * (bn ^ 2) * (G * (bn ^
2) - 2 * B - 1))
```

```
End Function
Option Explicit

Function Omega(ByVal h As Double, ByVal q As Double) As Double
   Omega = 1 - (1 - q) * h
End Function
```

```
Option Explicit

' h = e

Function STDErrPQ(ByVal f As Double, ByVal u As Double, ByVal h As Double, _
              ByVal p As Double, ByVal q As Double, _
              TArray As Variant, CArray As Variant) As Double
   Dim num_pts As Integer
   Dim w As Double
   Dim B As Double, G As Double
   Dim I As Integer, tao As Double, t As Double
   Dim cr_exp As Double, cr_th As Double
   Dim var As Double

   num_pts = Application.Count(TArray)

   w = Omega(h, q)
   B = p * f * w
   G = p * u
   var = 0

   For I = 0 To (num_pts - 1)
      tao = TArray(I)
      cr_exp = CArray(I)
      t = tao / w
      cr_th = ConcentrationRatio(G, B, t)
      var = var + (cr_th - cr_exp) ^ 2
   Next I

   STDErrPQ = (var / (num_pts - 1)) ^ 0.5

End Function

' h = e

Function STDErrPQ_SPRD(ByVal f As Double, ByVal u As Double, ByVal h As
Double, _
              ByVal p As Double, ByVal q As Double, _
              ByVal start_row As Integer, ByVal end_row As Integer, _
              ByVal start_column As Integer) As Double

   Dim num_pts  As Integer, I As Integer
   Dim TArray() As Double, CArray() As Double

   num_pts = end_row - start_row + 1
```

```
  ReDim TArray(num_pts - 1)
  ReDim CArray(num_pts - 1)

  For I = 0 To (num_pts - 1)
    TArray(I) = Cells(start_row + I, start_column)
    CArray(I) = Cells(start_row + I, start_column + 1)
  Next I

  STDErrPQ_SPRD = STDErrPQ(f, u, h, p, q, TArray, CArray)

End Function

Option Explicit

' h = e

Function STDErrQ(ByVal f As Double, ByVal u As Double, ByVal h As Double, _
                ByVal q As Double, _
                TArray As Variant, CArray As Variant) As Double
  Dim num_pts As Integer
  Dim w As Double
  Dim B As Double, G As Double
  Dim I As Integer, tao As Double, t As Double
  Dim cr_exp As Double, cr_th As Double
  Dim var As Double
  Dim p As Double

  num_pts = Application.Count(TArray)

  w = Omega(h, q)
  B = 3 * (1 / CArray(num_pts - 1) - 1)
  p = B / (f * w)
  G = p * u
  var = 0

  For I = 0 To (num_pts - 1)
    tao = TArray(I)
    cr_exp = CArray(I)
    t = tao / w
    cr_th = ConcentrationRatio(G, B, t)
    var = var + (cr_th - cr_exp) ^ 2
  Next I

  STDErrQ = (var / (num_pts - 1)) ^ 0.5

End Function
```

```
' h = e

Function STDErrQ_SPRD(ByVal f As Double, ByVal u As Double, ByVal h As Double,
_
                ByVal q As Double, _
                ByVal start_row As Integer, ByVal end_row As Integer, _
                ByVal start_column As Integer) As Double

   Dim num_pts  As Integer, I As Integer
   Dim TArray() As Double, CArray() As Double

   num_pts = end_row - start_row + 1
   ReDim TArray(num_pts - 1)
   ReDim CArray(num_pts - 1)

   For I = 0 To (num_pts - 1)
      TArray(I) = Cells(start_row + I, start_column)
      CArray(I) = Cells(start_row + I, start_column + 1)
   Next I

   STDErrQ_SPRD = STDErrQ(f, u, h, q, TArray, CArray)

End Function
```

REFERENCES

1. S. S. Wang, C. J. Lee and C. C. Chan, "Demulsification of water-in-oil emulsions by use of a high Voltage ac field," *Separation Science and Technology*, 29(2), pp. 159-170, 1994

2. J. Draxler, W. Furst and R. J. Marr, "Separation of metal species by emulsion liquid membrane," *Journal of Membrane Science*, Vol. 38, pp. 281-293, 1988

3. I. Abou-Nemeh and A. P. Van Peteghem, "Membrane recycling in the surfactant membrane process," *Ind. Eng. Chem. Res.*, vol. 32, pp. 1431-1437, 1993

4 J. Draxler and R. J. Marr. "Emulsion liquid membrane: part I, phenomenon and industrial application," *Chemical Engineering Process*, 20:319-329, 1986

5 D. Lorbach and R. J. Marr, "Emulsion liquid membrane: part II. modeling mass transfer of zinc with di(2-ethylhexyl) dithiophosphoric acid," *Chemical Engineering Process*, 21: 83-93, 1987

6 R. J. Marr, H. J. Bart, and J. Draxler, "Liquid membrane permeation," *Chemical Engineering Process*, 27:59-64, 1990

7 E. J. Fuller and N. N. Li. "Extraction of chromium and zinc from cooling tower blowdown by liquid membrane," *Journal of Membrane Science*, 18:251-271, 1984

8 R. J. Marr and A. Kopp, "Liquid membrane technology-a survey of phenomenon, mechanisms and models," *Int. Chem. Eng.*, 22(1):44-60, 1982

9 J. W. Frankenfield and N. N. Li, "Wastewater treatment by liquid ion exchange in liquid membrane systems," *Recent Development in Separation Science*, vol. 3, pp. 285-292, Boca Raton, FL, CRC Press, 1977

10 J. W. Frankenfield and N. N. Li, "Liquid membrane systems," *Ion Exchange for Pollution Control*, vol. 2, pp. 163-172, Boca Raton, FL, CRC Press, 1979

11 C. F. Reusch and E.I. Cussler, "Selective membrane transport," *AICHE J.* 19:736, 1973

12 D. K. SchifferC, A. M. Hochhauser, D. F. Evan and E.I. Cussler, "Concentrating solute with membrane containing carrirer," *Nature*, 250:484- 486, 1974

13 E. L. Cussler and D. F. Evans, "Liquid membrane for separation and reaction," *Journal of Membrane Science,* 6:113-121, 1980

14 R. A. Bartsch, W. A. Charewicz, S.I. Kang, and W. Walkowiak, "Proton-coupled transport of alkali metal cations across liquid membrane by ionized crown ethers, Liquid Membrane: Theory and Application," *ACS symp.* Ser. No. 347, pp. 86-97, 1987

15 W. Halwachs, E. Flaschel and K. Schugerl, "Liquid membrane transport-a highly selective separation process for organic solutes," Journal of Membrane Science, 6:33, 1980

16 R. E. Terry, N. N. Li and W. ho, "Extraction of phenolic compounds and organic acids by liquid membrane," *J. of Membrane Science,* 10:305-323, 1982

17 N. X. Yan, S. A. Huang, and Y. J. Shi, "Removal of acetic acid from wastewater with liquid surfactant membrane: an external boundary lager and membrane diffusion controlled model," *Separation Science Technology,* 22(2&3): 801- 818, 1987

18 X-L. Qian, X-S. Ma, and Y-J. Shi, "Removal of cyanide from wastewater with liquid membrane," *Water Treatment,* 4:99-111, 1989

19 M. P. Thien, T. A. Hatton and D.I.C. Wang, "Liquid emulsion membrane and their application in biochemical processing," *ACS Symp.* Ser. No. 314 pp. 67-77, 1986

20 W. Ho and R. M. Cowan, "Separation of latic acid from fermentation broth with liquid surfactant membrane," *the 194th ACS national meeting,* New Orleans, LA, September 1987

21 M. P. Thien, T. A. Hatton, "Liquid emulsion membrane and their application in biochemical processing," *Separation Science Technology,* 23(8&9): 819-853, 1988

22 N. N. Li and W. J. Asher, "Blood oxygenation by liquid membrane permeation, ACS Advances in Chemical Series, Chemistry Engineering in Medicine," *American Chemical Society,* New York, 1973

23 W. J. Asher, K. C. Bovee, J. W. Franken field, R.W. Hamilton, L. W. Henderson, P. C. Holtzapple and N. N. Li, "Liquid membrane system directed toward chronic uremia," *Kidney Int.* , Ser. No. 7, pp. 409, 1975

24 W. J. Asher, K. C. Bovee, J. W. Franken field, R.W. Hamilton, L. W. Henderson, P. C. Holtzapple and N. N. Li, "Liquid membrane system directed toward chronic uremia," *Kidney Int.* , Serial No. 10, pp. 254, 1976

25 W. J. Asher, K. C. Bovee, T.C. vogler, R.W. Hamilton, L. W. Henderson, P. C. Holtzapple, "Liquid membrane capsules for removal of urea from the blood," *Clin. Nephrol.,* 11:92, 1979

26 W. J. Asher, N. N. Li and A.L. Shirer, "Detoxifying-medical emulsion," *U.S. patent 4183918,* 1980

27 J. Draxler, R. J. Marr and M. Protsch, "Commercial-scale extraction of zinc by emulsion liquid membrane," *Separation Technology,* pp. 204-214, New York, 1988

28 X. J. Zhang, J. H. Liu and T. S. Lu, "Industrial application of liquid membrane separation for phenolic wastewater treatment," *Water Treatment,* 2:127-135, 1987

29 D. W. Zhou, "Emulsion liquid membrane removal of arsenic and strontium from wastewater," *Ph.D. dissertation,* Department of Chemical Engineering, Chemistry and Environmental Science, New Jersey Institute of Technology, Newark, New Jersey, 1996

30 S. A. El-Reefy, Y. T. Selium, and H. F. Aly, "Recovery of uranium from thorium in hydrochloric acid medium by liquid emulsion membranes containing trioctylphosphine oxide," *Journal of Radioanalytical and Nuclear Chemistry,* Vol. 228, NO. 1-2, pp. 21-25, 1998

31 C. J. Lee, S. S. Wang, and S. G. Wang, "Extraction of trivalent europium via emulsion liquid membrane containing PC-88A as mobile carrier," *Ind. Eng. Chem. Res.* Vol. 33, pp. 1556-1564, 1994

32 M. Goto, T. Kakoi, N. Yoshii, K. Kondo and F. Nakashio, "Effect of synthesized surfactants in the separation of rare earth metals by liquid surfactant membranes," *Ind. Eng. Chem. Res.* Vol. 32, pp. 1681-1685, 1993

33 J. M. T Vasconcelos and J. M. R Carvalho , Extraction of zinc by Alkyl Thiophosphoric Acid with emulsion liquid membranes," *Chem. Eng. Tech.* Vol. 16, pp. 213-217,1993

34 Mohammad S. Uddin and Kus Hidajat, "Extraction of gold from aqueous solution by carrier-mediated process using kryptofix 22 DD," *J. Chem. Tech. Biotechnol,* Vol. 58, pp. 123-128, 1993

35 R-S. Juang and R-H. Lo, "Effect of Acetate Medium on the extraction of cobalt(II) with di(2-ethylhexyl)phosphoric acid dissolved in Kerosene," *J. Chem. Tech. Biotechnol*, vol. 57, pp. 265-271, 1993

36 T. Huang and T. Tsai, "Separation of colbalt and nickel ions in lithium nitrate solutions by solvent extraction and liquid membrane with HEHEHP kerosene solution," *Acta Chemica Scandinavica*, vol. 45, pp. 383-391, 1991

37 P. J. Pickering and J. B. Chaudhuri, "Emulsion liquid membrane for chiral separations: selective extraction of rac-phenylalanine enantiomers," *Chirality*, vol. 9, pp. 261-267, 1997

38 I. Miesiac, K. Schugerl, A. Hasler, and J. Szymanowski, "Extraction and enzymatic hydrolysis of penicillin G in emulsion liquid membranes," *Journal of Radioanalytical and Nuclear Chemistry*, vol. 208, No. 1, pp.133-144, 1996

39 R. S. Juang and W.T. Huang, "Equilibrium studies on the extraction of citric acid from aqueous solutions with tri-n-octylamine," *Journal of Chemical Engineering of Japan*, vol. 27, No.4, 1994

40 N. N. Li, *US patent, 3410794(Nov. 12, 1968)*, 1968

41 T. Ohtake, T. Hano, K. Takagi, and F. Nakashio, "Effects of viscosity on drop a diameter of W/O emulsion dispersed in a stirred tank," J. Chem. Eng. Japan, 20(5): 443-447, 1987

42 R. Rautenbach and O. Machhammer, "Modeling of liquid membrane separation process," *Journal of Membrane Science*, 36: 425-444, 1988

43 W. S. Ho, "The size of liquid membrane emulsion globules in an agitating continuous phase: a dynamic measuring technique," *The 191st ACS national meeting and First international conference on Separation Science and Technology*, New York, April, 1986

44 E. S. Matulevicius and N. N. Li, Facilitated transport through liquid membrane," *Sep. Purif. Methods*, 4(1): 73-79, 1975

45 N. N. Li, "Facilitated transport through liquid membrane," *Journal of Membrane Science*, 3: 265, 1980

46 N. N. Li, "Encapsulated and Separation by liquid surfactant membrane," *Chemical Eng.*, 370: 325-327, 1981

47 R. D. Noble and J. D. Way, "Liquid membrane, Ion Exchange and Solvent Extraction, 10: 63-103, 1987

48 W. S. Ho, T. A. Hatton, E. N. Lightdoot and N. N. Li, "Batch extraction with liquid surfactant membrane: a diffusion control model," *AICHE J.* 28(4): 662-670, 1982

49 M. Teramoto, T. Sakai, K. Yanagann, M. Ohsuga and Y. Miyake, "Modeling of the permeation of copper through liquid surfactant membrane," *Separation Science Technology,* 18(8): 735-764, 1983

50 T. kataoka, T. Nishiki, S. Kimura and Y. Tomioka, "Batch permeation of metal ions using liquid surfactant membrane," *J. of Membrane Science,* 46: 67-80, 1989

51 S. C. Lee, B. S. Ahn and W. K. Lee, "Mathematical modeling of silver extraction by an emulsion liquid membrane process," *Journal of Membrane Science,* vol. 114, pp.171-185, 1996

52 K. C. Wang, "Mathematical modeling of emulsion liquid membrane systems," *Ph.D. Dissertation,* Department of Chemical Engineering, Chemistry and Environmental Science, New Jersey Institute of Technology, Newark, New Jersey, 1984

53 Rajdip Bardyopadhyaya, Avijit Bhowal, Siddhartha Datta and Shyamal K, Sanyal, "A new model of batch-extraction in emulsion liquid membrane: simulation of globule-globule interaction and leakage," *Chemical Engineering Science,* vol. 53, No. 15, pp. 2799-2807, 1998

54 J. H. Chang and W. K. Lee, "Modeling of enzymatic reaction with emulsion liquid membrane," *Chemical Engineering Science,* vol. 48, No. 13, pp. 2357-2366, 1993

55 M. Teramoto, H. Takihana, M. Shibutani, T. Yuasa and N. Hara, "Modeling of the permeation of copper through liquid surfactant membrane by continuous operation," *Separation Science Technology,* 18(11): 985-997, 1983b

56 F. D. Rumscheidt and S.G. Mason, "Particle motions in sheared suspension XI: internal circulation in fluid droplets." *J. Colloid. Science,* 16: 20, 1961

57 V.G. Levich, *Physiochemical Hydrodynamica,* Prentice Hall, Inc. Englewood, Cliffs, New Jersey, 1988

58 L. L. Tavlarides, C. A. Coulalogou, M. A. Zeitlin, G. E. Klinzing and B. Gal, "Bubble and drop phenomena," *Ind. Eng. Chem.,* 62: 6, 1970

59 J. W. Tester and M. Modell, *Thermodynamics and its applications,* Prentice Hall, Upper Saddle River, NJ, 1997

60 B. J. Raghuraman, N. P. Tirmizi and J. M. Wiencek, "Emulsion liquid membranes for wastewater treatment: equilibrium models for some typical metal-extractant systems," *Environmental Science & Technology,* vol. 28, No. 6, pp. 1090-1098, 1994

61 W. Lindsay, *Chemical Equilibria in Soils,* John Wiley and Sons, New York, 1979

62 K. S. Pitzer, *Thermodynamics,* Chapters 15-17, pp. 254-322, McGraw-Hill, New York, 3rd edition, 1995

63 B. J. Raghuraman, N. P. Tirmizi, B-S. Kim and J.M. Wiencek, "Emulsion liquid membranes for wastewater treatment: Equilibrium models for lead- and Cadmium-di-2-ethylhexyl phosphoric acid systems," *Environmental Science & Technology,* vol. 29, No. 4, pp. 979-984, 1995

64 L. A. Ajawin, E.S. Perez de Ortiz and H. Sawistowski, "Extraction of zinc by DI(2-Ethylhexyl) phosphoric acid," *Chemical Engineering Research and Design,* vol. 61, pp. 62-66, January 1983

65 F. Nakashio, M. Goto, M. Matsumoto, J. Irir and K. Kondo, "Role of surfactants in the behavior of emulsion liquid membrane: development of new sufactants," *Journal of Membrane Science,* 38: 249-260, 1988

66 F. Nakashio, "Recent advances in separation of metals by liquid surfactant membrane," *Journal of Chemical Engineering of Japan,* 26: 123, 1993

67 R-H. Zhang and L. Xiao, "Design of a liquid membrane system for extractin of rare earths," *Journal of Membrane Science,* 51(3): 249-258, 1990

68 C. R. Wilke and P. Chang, "Correlation of diffusion coefficients in diluent solutions," *AICHE Journal,* 1(2): 264, 1955

69 G. Les Bas, *The Molecular volume of liquid chemical compound,* Longmans, Green, New York, 1915

70 T. B. Jefferson, O. W. Witzell and W. L. Sibbett, "Thermal conductivity of graphite silicon oil and graphite-water separation," *Ing. Eng. Chem.,* 50: 1589, 1958

71 A. H. P Skelland and J. M. Lee, "Drop Size and continuous phase mass transfer in agitated vessels," *AICHE Journal,* 27(1): 99, 1981

72 D. R. Lide, *Handbook of Chemistry and Physics,* CRC Press, Boca Raton, New York, 78th Edition, 1997-1998